



Spontaneous magnon emission in the bosonic Klein paradox

Thesis by
Mexx Regout

First supervisor: Prof. Dr. R.A. Duine

Second supervisor: Prof. Dr. ir. H.T.C. Stoof

Daily supervisor: BSc. J. Harms

In Partial Fulfillment of the Requirements for the
Degree of
Theoretical Physics

UTRECHT UNIVERSITY
Utrecht, Netherlands

2022

ACKNOWLEDGEMENTS

I would like to thank Rembert Duine and Joren Harms for their extensive support over the last year in my thesis work. A lot of insightful conversations and lessons were obtained from them and I couldn't have done this without their help. I also want to thank Henk Stoof for being my second supervisor and Artim Bassant for the support and helpful remarks over the year.

ABSTRACT

We show how the quantum mechanical treatment of magnon-antimagnon coupling leads to the enhancement of magnonic spin current analogous to the bosonic Klein paradox. In addition to this we investigate the scattering dynamics of this magnonic system resulting in a description of spontaneous magnon emission in an in-state vacuum. The spontaneous emission will then be compared to thermal emission to get a critical temperature which entails measurability.

TABLE OF CONTENTS

Acknowledgements	2
Abstract	3
Table of Contents	4
Chapter I: Introduction	5
Chapter II: Setting up the Klein Paradox for Spin Waves	7
Chapter III: Energy spectrum	10
3.1 Magnon Quantization in the Left Metal	10
3.2 Antimagnon Quantization in the Right Metal	16
3.3 Magnonic Wavenumbers	18
3.4 Equation of Motion for the Momentum Operators	19
3.5 The Bogoliubov Transformation	20
Chapter IV: Coupling the Magnon and Antimagnon Region	22
4.1 Boundary Conditions	22
4.2 The M-matrix	25
Chapter V: Scattering Dynamics	28
5.1 Scattering States	28
5.2 In and Out States	31
5.3 Conserved Probability Current	32
5.4 Solving the S Matrix	33
Chapter VI: Spontaneous magnonic emission	37
6.1 Magnonic Particle Numbers	37
6.2 Thermal in-states	38
Chapter VII: Conclusion and outlook	41
7.1 Conclusion	41
7.2 Outlook	41
Appendix A: Bogoliubov momentum modes	42
Appendix B: Scattering states	44
Bibliography	47

Chapter 1

INTRODUCTION

In the field of quantum mechanics there are certain intrinsic properties for fundamental particles. One such intrinsic property is the spin. This spin attributes for example to the intrinsic magnetic dipole moment of an electron. These spins can be arranged in a periodic lattice where all the spins align. In order to keep the spins aligned it is possible to introduce a so called exchange constant. This exchange constant, when positive, ensures that anti-alignment between spins on the lattice results in a higher unstable total energy than the preferred ground state energy. This setup of aligned spins is called ferromagnetic since there is a collectively positive magnetic dipole moment on the lattice. With the introduction of an external magnetic field on the spins in the lattice we get Larmor precession of the spin. This precession can be disturbed by some external driving or thermal fluctuations. Because all the spins in the lattice are trying to align with each other we get that the disturbance will propagate through the spin lattice setup. This propagation of reordering spin directions is called a spin wave. In figure 1.1 it is shown what such a spin wave would look like.

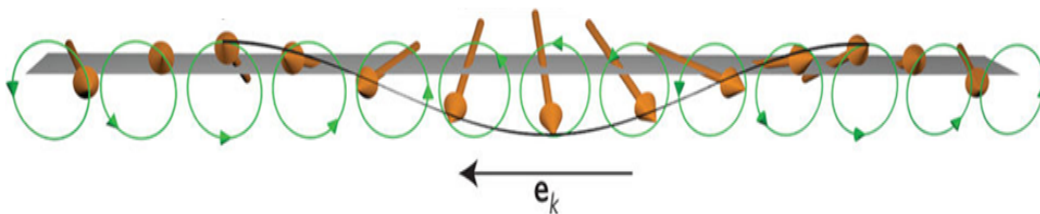


Figure 1.1: Spin wave moving to the left. The green circles are the Larmor precession with the orange arrows indicating the spin direction. Figure is from [7].

In figure 1.1 we see the black line moving along the spin tips illustrating the spin wave due to the external driving or thermal fluctuations. When one quantizes such a spin wave, to be a wave packet, we get a so called magnon. There are also antimagnons which are similar to magnons except for the fact

that the spins are anti-aligned with the external magnetic field as we will see in chapter 2. These magnons are a fundamental part of the field of magnonics. This field utilizes the spin degree of freedom to create improvements in for example electronic devices. One of the problems with electronic devices is that Joule heating occurs due to friction between the electron current and the constituents of the conductor itself. This Joule heating doesn't occur when magnons are used as a means of transmitting information. Magnons could thus lead to potentially more energy efficient devices. One of the challenges however with magnons is that they decay rather fast due to dissipation. This makes it harder to apply magnons in devices with it's short decay length. A possible solution for this problem would be a magnon amplifier to overcome the loss of signal by dissipation. The question then arises how such a magnon amplifier could be constructed.

The inspiration for a solution comes from the bosonic Klein paradox. In this so called paradox it arises from the Dirac equation that it is possible to get amplified reflection from a potential wall for bosons. This amplified reflection comes from the fact that there is particle/anti-particle creation at the boundary. The idea of a magnonic analogue of the bosonic Klein paradox found it's way into the paper, "Enhanced magnon spin current using the bosonic Klein paradox", by Harms et al [2]. In this paper there is a coupling of magnons to antimagnons leading to enhanced magnon spin currents.

In this thesis the goal is to re-derive some of the results from [2] in a quantum mechanical treatment of the magnonic analogue of the Klein paradox. After that is done it will be possible to set up the scattering dynamics in the form of the scattering matrix S . This in turn allows for the study of spontaneous magnon emission from the boundary with vacuum and thermal states.

Chapter 2

SETTING UP THE KLEIN PARADOX FOR SPIN WAVES

In this chapter there will be an overview of the elements needed to create a stable magnon-antimagnon setup in a classical way. This setup will then be mimicked in chapter 3 for the quantum mechanical treatment of the magnonic Klein paradox. So let's take a closer look at this magnon/antimagnon setup. Figure 2.1 shows what the system setup might look like.

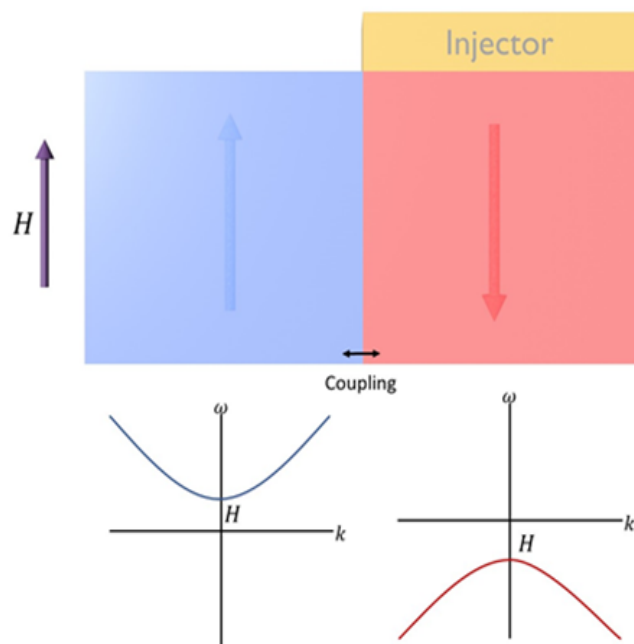


Figure 2.1: Magnon/antimagnon system setup with the blue spins aligning with the external magnetic field H and the red spins anti-aligning with H . The magnon and antimagnon dispersion's are shown below without the effect of the injector incorporated on the right.

What we see in figure 2.1 is that the dispersion on the left indicates a stable state for the magnons. The antimagnons on the right are in a meta stable state. The lowest energy configuration for the spins on the right would be alignment with the external magnetic field H . It is therefore needed to have

some additional force working on the anti-aligned spins to keep them dynamically stable. This is what the injector in the right section of figure 2.1 will facilitate. This injector works by inducing a spin orbit torque on the anti-aligned spins. This torque will keep the spins anti-aligned with the external magnetic field by overcoming the Gilbert damping. Figure 2.2 shows how this spin orbit torque arises in the injector.

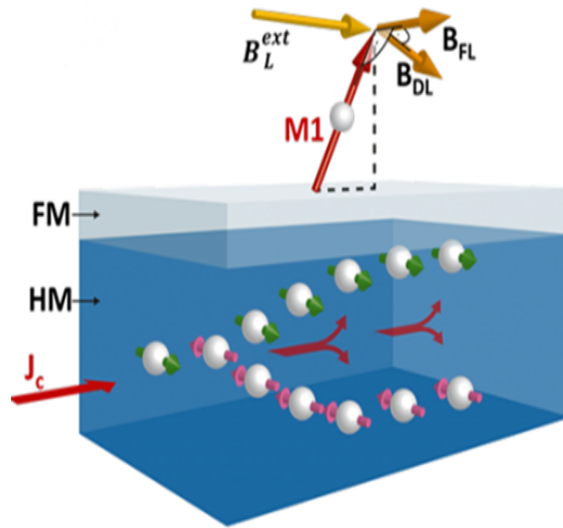


Figure 2.2: The damping like force B_{DL} in the ferromagnetic layer (FM) is induced by the charge current J_c in the heavy metal layer (HM) via spin orbit coupling. This B_{DL} compensates for the Gilbert damping and thus stabilizes the anti-aligned spins. This figure is adapted from [8].

When we combine the injector which induces spin orbit torque with the ferromagnetic magnon/antimagnon regions we arrive at the schematic setup used in the paper by Harms et al.

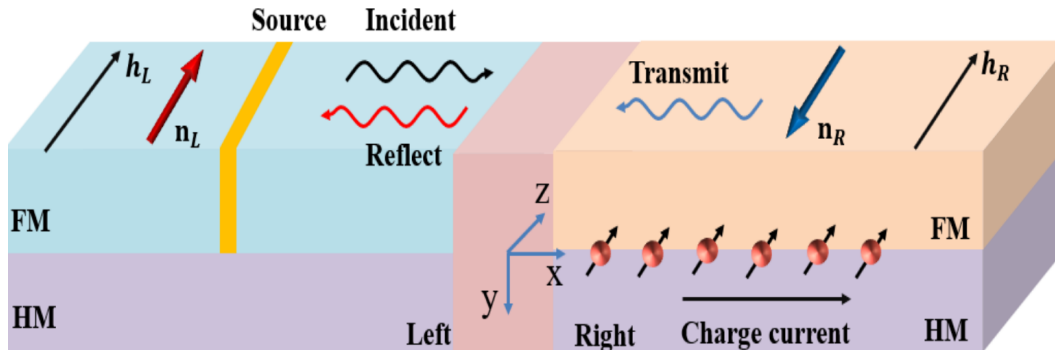


Figure 2.3: Bosonic Klein paradox setup from [2]. In the left FM region we have the alignment of spins with the external magnetic field h_L . In the right FM region we have the anti-alignment of spins with the external magnetic field h_R which is maintained by the charge current in the HM layer on the right

In figure 2.3 we see an example of an scattering event with incoming and outgoing magnonic excitation's which we will study in chapter 5. The setup given in figure 2.3 will be applied in chapter 3 for the modeling of the Hamiltonian's

Chapter 3

ENERGY SPECTRUM

In this chapter we will show how to derive the quantum mechanical Hamiltonian's for (anti)magnons which describe the system given in figure 2.3. This will be done by transforming the ferromagnetic spin Hamiltonian into (anti)magnon Hamiltonian's via the Holstein-Primakoff transformation. These Hamiltonian's will enable us to derive the dispersion relation's of the bulk for the (anti)magnon states. These dispersion's will give us insight into the types of modes that can be expected in the system when looking at specific energies. We will also introduce some useful concepts like the Heisenberg equation of motion and the Bogoliubov transformation in preparation of chapter 4.

3.1 Magnon Quantization in the Left Metal

To start with the derivation of the magnon Hamiltonian on the left it will be necessary to first define the Hamiltonian of the ferromagnetic spin chain with a transverse magnetic field on the left. This is done as follows

$$\hat{\mathcal{H}}_L = -J \sum_{\langle i,j \rangle} \vec{\hat{S}}_{i,L} \cdot \vec{\hat{S}}_{j,L} - \sum_i \vec{B}_L \cdot \vec{\hat{S}}_{i,L}. \quad (3.1)$$

Here $J > 0$ represents the ferromagnetic exchange coupling between spins. $\vec{\hat{S}}_{i,L} = (\hat{S}_{i,L}^x, \hat{S}_{i,L}^y, \hat{S}_{i,L}^z)$ is the spin operator vector at site i . The vector \vec{B}_L is the direction and magnitude of the transverse magnetic field in the left metal. The Hamiltonian is designed in such a way that spin alignment with the external magnetic field is the lowest possible energy state.

The Hamiltonian in (3.1) uses spin vector operators. To describe magnons it will be useful to use operators which describe a quantized spin fluctuation around some classical minimum. In order to do this it is necessary to first define the basis vectors and the spin raising and lowering operators for the system. The basis vectors will be $(\vec{e}_1, \vec{e}_2, \vec{\Omega}_{cl})$ where the following relation holds for $\vec{\Omega}_{cl}$, from section 11.2 in [1].

$$\vec{e}_1 \times \vec{e}_2 = \vec{\Omega}_{cl}, \quad (3.2)$$

where the cross implies the vector cross product. $\vec{\Omega}_{cl}$ is the axis which classically minimizes the spin Hamiltonian. The definition of the raising and lowering operators for the spin, from section 11.2 in [1], are as follows

$$S_i^\pm = \vec{S}_i \cdot \vec{e}_1 \pm i\vec{S}_i \cdot \vec{e}_2. \quad (3.3)$$

We can define the magnon operators, also known as Holstein-Primakoff operators (from section 11.2 in [1]), with the definitions from (3.2) and (3.3) as follows

$$\begin{aligned} \hat{S}_{i,L}^+ &= \sqrt{2S - \hat{n}_{i,L}} \hat{\psi}_{i,L}, \\ \hat{S}_{i,L}^- &= \hat{\psi}_{i,L}^\dagger \sqrt{2S - \hat{n}_{i,L}}, \\ \vec{S}_{i,L} \cdot \vec{\Omega}_{cl}^L &= -\hat{n}_{i,L} + S, \end{aligned} \quad (3.4)$$

where S is the total spin per site. $\hat{n}_i = \hat{\psi}_{i,L}^\dagger \hat{\psi}_{i,L}$ is the magnonic occupation number operator, $\hat{\psi}_{i,L}$ the annihilation and $\hat{\psi}_{i,L}^\dagger$ the creation operator for the magnons. These operators obey the bosonic commutation relations $[\hat{\psi}_{i,L}, \hat{\psi}_{j,L}^\dagger] = \delta_{ij}$ and $[\hat{\psi}_{i,L}, \hat{\psi}_{j,L}] = [\hat{\psi}_{i,L}^\dagger, \hat{\psi}_{j,L}^\dagger] = 0$.

These bosonic commutation relations ensure that the definitions made in (3.4) satisfy the spin commutation relations (from section 7.1 in [1]), $[\hat{S}^\alpha, \hat{S}^\beta] = i\epsilon^{\alpha\beta\gamma} \hat{S}^\gamma$, where $\epsilon^{\alpha\beta\gamma}$ is the Levi-Civita symbol with $\alpha, \beta, \gamma \in \{x, y, z\}$. For the magnon Hamiltonian on the left we use the following definitions for the basis vectors and magnetic field vector: $\vec{e}_1 = (1, 0, 0)$, $\vec{e}_2 = (0, 1, 0)$, $\vec{\Omega}_{cl} = (0, 0, 1)$ and $\vec{B}_L = (0, 0, h_L)$.

With these definitions it is possible to rewrite the spin Hamiltonian $\hat{\mathcal{H}}_L$ from (3.1) in terms of magnon operators as follows

$$\begin{aligned} \hat{\mathcal{H}}_{L,M} &= -J \sum_{\langle i,j \rangle} \vec{S}_i \cdot \vec{S}_j - h_L \sum_i S_i^z, \\ &= -J \sum_{\langle i,j \rangle} \left\{ \frac{1}{2} \hat{\psi}_i^\dagger \sqrt{2S - \hat{n}_i} \sqrt{2S - \hat{n}_j} \hat{\psi}_j + \frac{1}{2} \sqrt{2S - \hat{n}_i} \hat{\psi}_i \hat{\psi}_j^\dagger \sqrt{2S - \hat{n}_j} \right. \\ &\quad \left. - S(\hat{n}_i + \hat{n}_j) + \hat{n}_i \hat{n}_j \right\} - h_L \sum_i (-\hat{n}_i + S) - JS^2 \mathcal{N}, \\ &\simeq -J \sum_{\langle i,j \rangle} S \{ \hat{\psi}_i^\dagger \hat{\psi}_j + \hat{\psi}_i \hat{\psi}_j^\dagger \} - S(\hat{n}_i + \hat{n}_j) + h_L \sum_i \hat{n}_i - h_L S \mathcal{N} - JS^2 \mathcal{N}. \end{aligned} \quad (3.5)$$

The definitions from (3.3) and (3.4) are used to arrive at the second equality in (3.5). In that equality we represent the total number of sites as \mathcal{N} . The last line in (3.5) was derived by applying the approximation $S \gg \langle \hat{n}_i \rangle$ in combination with only considering operators up to quadratic order. The physical meaning behind S being much larger than the magnonic occupation number is that we only consider small spin fluctuations with respect to the z-axis. The approximation about the operator order comes from the fact that we only want to study non-interacting spin waves in this setup.

The Hamiltonian derived in (3.5) can be further expanded by taking the nearest neighbour approximation between the magnon operators with the following equality

$$\sum_{\langle i,j \rangle} \hat{\psi}_i^\dagger \hat{\psi}_j + \hat{\psi}_i \hat{\psi}_j^\dagger = \frac{1}{2} \sum_i \sum_{j=\pm a} \hat{\psi}_i^\dagger \hat{\psi}_{i+j} + \hat{\psi}_i \hat{\psi}_{i+j}^\dagger, \quad (3.6)$$

where a is the lattice spacing between two sites and the factor of $\frac{1}{2}$ is included to prevent over counting. When we apply the nearest neighbour approximation in (3.6) to the final line in (3.5) we end up with the following Hamiltonian

$$\begin{aligned} \hat{\mathcal{H}}_{L,M} = & -\frac{JS}{2} \sum_i \sum_{j=\pm a} \{ \hat{\psi}_i^\dagger \hat{\psi}_{i+j} + \hat{\psi}_i \hat{\psi}_{i+j}^\dagger \} + 2JS \sum_i \hat{n}_i + h_L \sum_i \hat{n}_i - h_L S \mathcal{N} \\ & - JS^2 \mathcal{N}. \end{aligned} \quad (3.7)$$

In order to get the dispersion from equation (3.7) it is necessary to introduce the Fourier transformation of the creation/annihilation operators. The Fourier transformation for the operators is together with the Kronecker delta defined below

$$\hat{\psi}_{j,t} = \frac{1}{\sqrt{\mathcal{N}}} \sum_k e^{-i\omega_k t} e^{ikx_j} \hat{\psi}_k, \quad (3.8a)$$

$$\hat{\psi}_{j,t}^\dagger = \frac{1}{\sqrt{\mathcal{N}}} \sum_k e^{i\omega_k t} e^{-ikx_j} \hat{\psi}_k^\dagger, \quad (3.8b)$$

$$\mathcal{N} \delta_{k,k'} = \sum_j e^{i(k-k')x_j}, \quad (3.8c)$$

where $x_j = aj$, with lattice constant a and $j \in \mathbb{N}$. The commutation relations for the Fourier transformed operators is $[\hat{\psi}_k, \hat{\psi}_{k'}^\dagger] = \delta_{k,k'}$ for magnons. The identities in (3.8a) and (3.8b) can be inserted into (3.7) to derive the dispersion

for the magnons.

$$\begin{aligned}
\hat{\mathcal{H}}_{L,M} &= -\frac{JS}{2\mathcal{N}} \sum_i \sum_{j=\pm a} \sum_{k,k'} \{e^{-ik'x_i} \hat{\psi}_{k'}^\dagger e^{ikx_{i+j}} \hat{\psi}_k + e^{ik'x_i} \hat{\psi}_{k'} e^{-ikx_{i+j}} \hat{\psi}_k^\dagger\} \\
&\quad + (2JS + h_L) \sum_i \sum_{k,k'} e^{i(k-k')x_i} \hat{\psi}_k^\dagger \hat{\psi}_{k'} - h_L S \mathcal{N} - JS^2 \mathcal{N}, \\
&= \sum_k \{2JS(1 - \cos(ka)) + h_L\} \hat{\psi}_k^\dagger \hat{\psi}_k + \alpha, \\
&= \sum_k \omega_k^L \hat{\psi}_k^\dagger \hat{\psi}_k + \alpha \equiv \hat{H}_{L,M} + \alpha.
\end{aligned} \tag{3.9}$$

The identity in equation (3.8c) was applied to the first equality in (3.9) to get the second equality. We describe the magnon excitation's in the following Hamiltonian: $\hat{H}_{L,M} = \sum_k \omega_k^L \hat{\psi}_k^\dagger \hat{\psi}_k$. The magnon dispersion of the bulk on the left is $\omega_k^L = 2JS(1 - \cos(ka)) + h_L$. The constant $\alpha \equiv -JS \sum_k \cos(ka) - S\mathcal{N}(h_L + JS)$. We can take the limit of the lattice constant going to zero such that we get to a continuous field theory description instead of a discrete lattice model

$$\omega_M^L(k) \equiv \lim_{a \rightarrow 0} \omega_k^L = JSa^2 k^2 + h_L. \tag{3.10}$$

This is the continuous dispersion of the magnons on the left.

The magnons are not the only possible modes within this setup. We can also introduce the antimagnons. The antimagnons fluctuate around the negative z-axis instead of the positive z-axis for magnons. The definition of a creation and annihilation operator is inverted for antimagnons with respect to magnons. The creation of a magnon has the same effect as the annihilation of an antimagnon and vice versa. because of this we need to treat the HPT transformation with care when we look at the antimagnon description of it.

So the Holstein-Primakoff transformation for antimagnons is now defined as follows

$$\begin{aligned}
\hat{S}_{i,L}^+ &= \hat{\psi}_{i,L}^\dagger \sqrt{2S - \hat{n}_{i,L}}, \\
\hat{S}_{i,L}^- &= \sqrt{2S - \hat{n}_{i,L}} \hat{\psi}_{i,L}, \\
\hat{S}_{i,L}^z &= -\hat{n}_{i,L} + S,
\end{aligned} \tag{3.11}$$

with the antimagnon occupation number $\hat{n}_{i,L} = \hat{\psi}_{i,L} \hat{\psi}_{i,L}^\dagger$. The antimagnons obey the following bosonic commutation relations: $[\hat{\psi}_{i,L}, \hat{\psi}_{j,L}^\dagger] = -\delta_{i,j}$ and

$[\hat{\psi}_{i,L}, \hat{\psi}_{j,L}] = [\hat{\psi}_{i,L}^\dagger, \hat{\psi}_{j,L}^\dagger] = 0$. When we take the same approach to $\hat{\mathcal{H}}_L$ with the definitions from (3.11) it follows that the Hamiltonian for the antimagnon excitation's has the following form

$$\hat{H}_{L,AM} = \sum_k \omega_k^L \hat{\psi}_k \hat{\psi}_k^\dagger, \quad (3.12)$$

with the same ω_k^L as in $\hat{H}_{L,M}$. The key difference between the magnon/antimagnon approach is the commutation relation of the operators. To see the effect of the commutation relations we have to look at the Heisenberg equations of motion. The Heisenberg equation of motion is defined, in chapter 3 from [6], as follows

$$-i\hbar\partial_t\hat{\Psi} = [\hat{H}, \hat{\Psi}], \quad (3.13)$$

where $\hat{\Psi}$ can be any of the creation/annihilation operator like the operators given in the Holstein-Primakoff transformations. The constant \hbar will equal one for the rest of the thesis except in section 6.2 about thermal in-states. We can determine the equation of motion of $\hat{\psi}_{j,t}$ on the left for both the magnon and antimagnon commutation relation and quantization. So we start with the equation of motion for magnons with $[\hat{\psi}_i, \hat{\psi}_j^\dagger] = \delta_{i,j}$ as shown below.

$$\begin{aligned} -i\partial_t\hat{\psi}_{j,t} &= [\hat{\mathcal{H}}_{L,M}, \hat{\psi}_{j,t}], \\ -i\partial_t \sum_k e^{-i\omega_{k,M}^L t} e^{ikx_j} \frac{\hat{\psi}_k}{\sqrt{\mathcal{N}}} &= \left[\sum_{k'} \omega_{k'}^L \hat{\psi}_{k'}^\dagger \hat{\psi}_{k'}, \sum_k e^{-i\omega_{k,M}^L t} e^{ikx_j} \frac{\hat{\psi}_k}{\sqrt{\mathcal{N}}} \right], \\ \sum_k (-\omega_{k,M}^L) e^{-i\omega_{k,M}^L t} e^{ikx_j} \frac{\hat{\psi}_k}{\sqrt{\mathcal{N}}} &= \sum_k (-\omega_k^L) e^{-i\omega_{k,M}^L t} e^{ikx_j} \frac{\hat{\psi}_k}{\sqrt{\mathcal{N}}}. \end{aligned} \quad (3.14)$$

In (3.14) we applied the Fourier transform from (3.8a) and $[\hat{\psi}_k, \hat{\psi}_{k'}^\dagger] = \delta_{k,k'}$. From the derivation shown in (3.14) we conclude that $\omega_{k,M}^L = \omega_k^L$ as was already chosen to be the case in the discrete version of equation (3.10). We can do the same procedure for the antimagnons with $[\hat{\psi}_i, \hat{\psi}_j] = -\delta_{i,j}$ as seen below.

$$\begin{aligned} -i\partial_t\hat{\psi}_{j,t} &= [\hat{\mathcal{H}}_{L,AM}, \hat{\psi}_{j,t}], \\ -i\partial_t \sum_k e^{i\omega_{k,AM}^L t} e^{ikx_j} \frac{\hat{\psi}_k}{\sqrt{\mathcal{N}}} &= \left[\sum_{k'} \omega_{k'}^L \hat{\psi}_{k'} \hat{\psi}_{k'}^\dagger, \sum_k e^{i\omega_{k,AM}^L t} e^{ikx_j} \frac{\hat{\psi}_k}{\sqrt{\mathcal{N}}} \right], \\ \sum_k (-\omega_{k,AM}^L) e^{i\omega_{k,AM}^L t} e^{ikx_j} \frac{\hat{\psi}_k}{\sqrt{\mathcal{N}}} &= \sum_k (\omega_k^L) e^{i\omega_{k,AM}^L t} e^{ikx_j} \frac{\hat{\psi}_k}{\sqrt{\mathcal{N}}}. \end{aligned} \quad (3.15)$$

We applied the Fourier transform from (3.8a) to (3.15) with $[\hat{\psi}_k, \hat{\psi}_{k'}^\dagger] = -\delta_{k,k'}$. From the derivation shown in (3.15) we conclude that $\omega_{k,AM}^L = -\omega_k^L$. In

section 3.4 we will revisit the equation of motion for the momentum operators $\hat{\psi}_{L/R}(k, t)$.

From the equations in (3.14) and (3.15) we see that the antimagnon states are the negative energy counterparts of the magnon states. This results in the following continuous dispersion for the antimagnons on the left

$$\omega_{AM}^L(k) = -JSa^2k^2 - h_L. \quad (3.16)$$

Both magnon and antimagnon dispersion's are shown in figure 3.1.

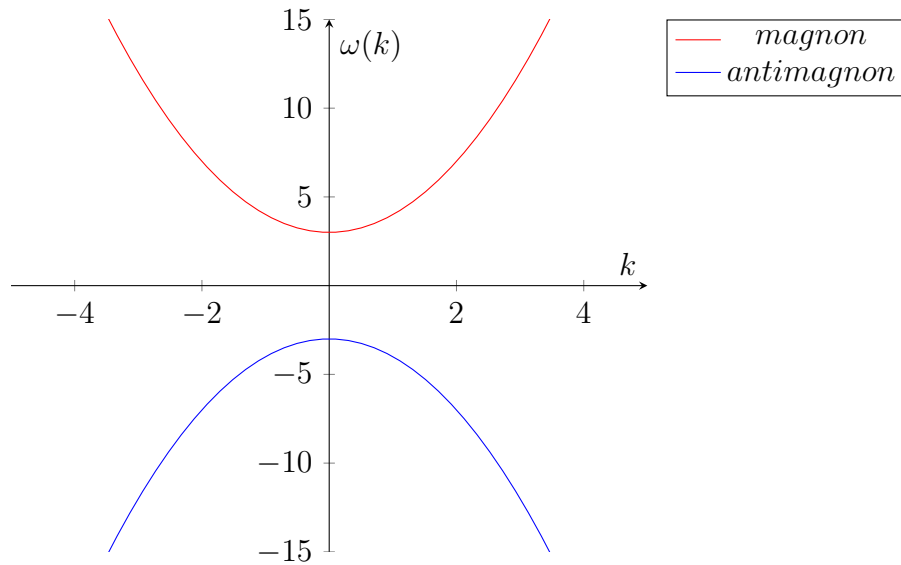


Figure 3.1: Dispersion's for both magnons and antimagnons in the left metal at the value of $h_L = 3$.

In figure 3.1 we see that the magnon dispersion reflects a stable mode within the left metal. The antimagnon dispersion however diverges to negative infinity with increasing momentum k . This dispersion displays the meta stable nature of the antimagnon excitation's in the left metal and are thus not present for $\omega > 0$.

3.2 Antimagnon Quantization in the Right Metal

The approach for the magnon/antimagnon quantization in the right metal goes fairly analogous to the left metal quantization. The crucial difference will be that in the right metal the classical minimization axis $\vec{\Omega}_{cl}^R$ will be the negative z axis. This is the manifestation of the spin orbit torque in our treatment of the Hamiltonian on the right. In order to get $\vec{\Omega}_{cl}^R = (0, 0, -1)$ it will be necessary to define the basis vectors as $\vec{e}_1 = (1, 0, 0)$ and $\vec{e}_2 = (0, -1, 0)$. The following Holstein-Primakoff transformation will be used for the right metal

$$\begin{aligned}\hat{S}_{i,R}^+ &= \sqrt{2S - \hat{n}_{i,R}} \hat{\psi}_{i,R}, \\ \hat{S}_{i,R}^- &= \hat{\psi}_{i,R}^\dagger \sqrt{2S - \hat{n}_{i,R}}, \\ \hat{S}_{i,R}^z &= \hat{n}_{i,R} - S,\end{aligned}\tag{3.17}$$

where $\hat{n}_{i,R} = \hat{\psi}_{i,R}^\dagger \hat{\psi}_{i,R}$ is the occupation number for the magnons. $\hat{\psi}_{i,R}^\dagger$ is the creation and $\hat{\psi}_{i,R}$ the annihilation operator for the magnons. The magnons obey the following bosonic commutation relations: $[\hat{\psi}_{i,R}, \hat{\psi}_{j,R}^\dagger] = \delta_{i,j}$ and $[\hat{\psi}_{i,R}, \hat{\psi}_{j,R}] = [\hat{\psi}_{i,R}^\dagger, \hat{\psi}_{j,R}^\dagger] = 0$. Just like in the left metal we have the inverse quantization for the antimagnons on the right which obeys the bosonic commutation relations: $[\hat{\psi}_{i,R}, \hat{\psi}_{j,R}^\dagger] = -\delta_{i,j}$ and $[\hat{\psi}_{i,R}, \hat{\psi}_{j,R}] = [\hat{\psi}_{i,R}^\dagger, \hat{\psi}_{j,R}^\dagger] = 0$.

The ferromagnetic Hamiltonian with transverse magnetic field in the right metal has the following form

$$\hat{\mathcal{H}}_R = -J \sum_{\langle i,j \rangle} \vec{\hat{S}}_{i,R} \cdot \vec{\hat{S}}_{j,R} - \sum_i \vec{B}_R \cdot \vec{\hat{S}}_{i,R}.\tag{3.18}$$

We take the magnetic field to be in the same direction as \vec{B}_L with a different magnitude resulting in $\vec{B}_R = (0, 0, h_R)$. This magnetic field vector can be applied to equation (3.18) to get

$$\hat{\mathcal{H}}_R = -J \sum_{\langle i,j \rangle} \vec{\hat{S}}_{i,R} \cdot \vec{\hat{S}}_{j,R} - h_R \sum_i \hat{S}_{i,R}^z.\tag{3.19}$$

From equation (3.19) we can derive the Hamiltonian's for the magnon and antimagnon excitations in the right metal analogously to what is done in section 3.1. These excitation Hamiltonian's are as follows

$$\hat{H}_{R,M} = \sum_k \omega_k^R \hat{\psi}_k^\dagger \hat{\psi}_k,\tag{3.20a}$$

$$\hat{H}_{R,AM} = \sum_k \omega_k^R \hat{\psi}_k \hat{\psi}_k^\dagger,\tag{3.20b}$$

where $\omega_k^R = 2JS(1 - \cos(ka)) - h_R$. When we take the lattice constant to zero we get the continuous dispersion for the magnons/antimagnons in the right metal

$$\omega_{M/AM}^R(k) = \pm(JSa^2k^2 - h_R), \quad (3.21)$$

where plus represents the magnon modes and minus the antimagnon modes. The dispersion's are shown in figure 3.2.

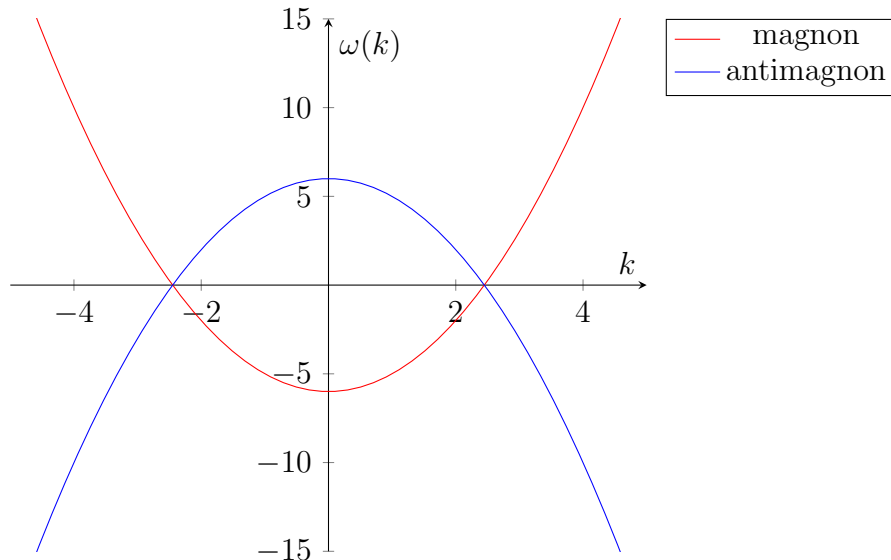


Figure 3.2: Dispersion's for both magnons and antimagnons in the right metal at $h_R = 6$.

In figure 3.1 we saw two non overlapping dispersion's. In figure 3.2 we see that the dispersion of the magnons is shifted down and the antimagnons is shifted upwards with respect to the dispersion's in the left metal. This is due to the inversion of the classical minimization axis in the Holstein-Primakoff transformation. With this upward shift for the antimagnon dispersion we see that there are antimagnon excitations present for $\omega > 0$. In figure 3.3 we see all the magnonic excitations together.

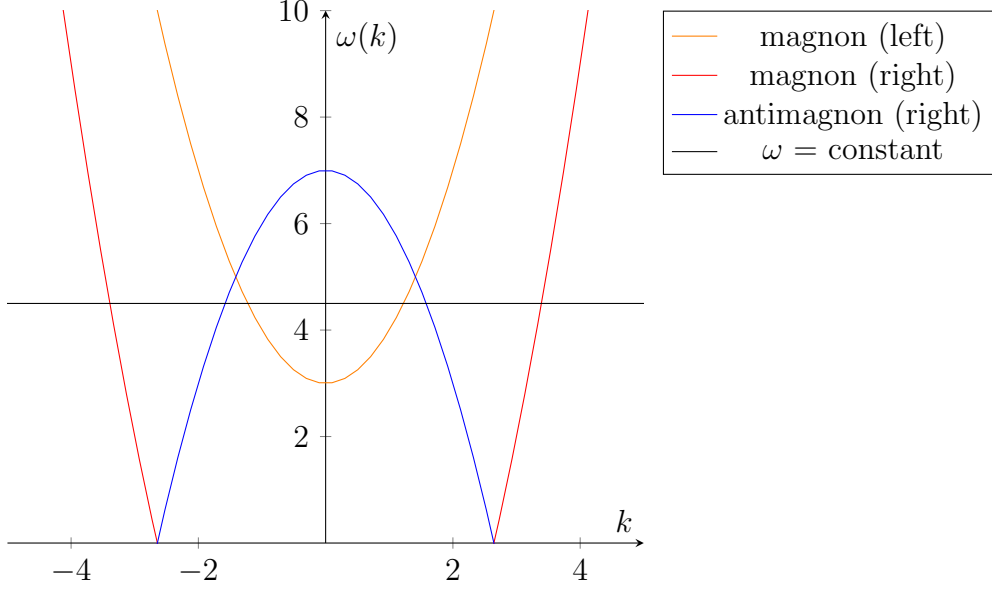


Figure 3.3: Dispersion's for magnons and antimagnons from both metals at $h_L = 3$ and $h_R = 7$. Only the region $\omega > 0$ is shown.

Figure 3.3 shows that for certain value's of ω we get coexistence of magnon modes left and magnon/antimagnon modes on the right in the $\omega > 0$ region. For $\omega \in \{h_L, h_R\}$ we have four magnon modes and two antimagnon modes in the system. This region for ω will be of interest since we want to create a system such that we can couple a magnonic region with an antimagnonic region. In section 3.3, about magnonic wavenumbers, it will be made more explicit what momenta these modes can have. We will also see in that section if the antimagnon dispersion in the left metal is present in any way.

3.3 Magnonic Wavenumbers

With the dispersion's derived in the previous section it is possible to determine the wavenumbers of the magnon and antimagnon modes at a fixed ω .

For $\omega > \omega_{min} \equiv h_L$, in the left magnet, we find two real k_r^L, k_t^L and two complex k_+^L, k_-^L wavenumbers given by

$$\Lambda k_{r/l}^L = \pm \sqrt{\omega - h_L}, \quad \Lambda k_{+/-}^L = \pm i \sqrt{\omega + h_L}, \quad (3.22)$$

where $\Lambda^2 = JSa^2$. When we inspect the complex wavenumbers we see that, in the Fourier expansion of ψ_L , one blows up and the other is damped. The exponentially damped modes are physically allowed while the growing mode

will be excluded later on since they are not physical. In the right magnet, for $\omega < \omega_{max} \equiv h_r$, there are four real wavenumbers

$$\Lambda k_{r/l}^R = \pm \sqrt{\omega + h_R}, \quad \Lambda k_{+/-}^R = \pm \sqrt{h_R - \omega}, \quad (3.23)$$

where $k_{r/l}^R$ correspond to the magnon modes and $k_{+/-}^R$ to the antimagnon modes. These wave numbers will later be used in the section about the M-matrix, see section 4.2.

3.4 Equation of Motion for the Momentum Operators

In section 4.2 we will determine the Bogliubov momentum modes in equation (4.17). In order to do this we need to know the constraint on these momentum modes. These modes are constraint by the equation of motion and commutation relation of $\hat{\psi}_{L/R}(k, t)$. So we can use equation (3.13) to derive the conditions that are needed to be satisfied for $\psi_{L/R}(k, t)$. The magnon equation of motion on the left is shown in equation (3.24)

$$\begin{aligned} -i\partial_t \hat{\psi}_L(k', t) &= [\hat{\mathcal{H}}_{L,M}, \hat{\psi}_L(k', t)], \\ &= \left[\int dk \omega^L(k) \hat{\psi}_L^\dagger(k, t) \hat{\psi}_L(k, t), \hat{\psi}_L(k', t) \right], \\ &= \int dk \omega^L(k) [\hat{\psi}_L^\dagger(k, t) \hat{\psi}_L(k, t) \hat{\psi}_L(k', t) - \hat{\psi}_L(k', t) \hat{\psi}_L^\dagger(k, t) \hat{\psi}_L(k, t)], \\ &= -\omega^L(k') \hat{\psi}_L(k', t), \end{aligned} \quad (3.24)$$

where we used $[\hat{\psi}_L(k), \hat{\psi}_L^\dagger(k')] = \delta(k - k')$ and the continuous magnon Hamiltonian with $\omega^L(k) = JSa^2k^2 + h_L$. The antimagnon equation of motion on the right is shown in equation (3.25)

$$\begin{aligned} -i\partial_t \hat{\psi}_R(k', t) &= [\hat{\mathcal{H}}_{R,AM}, \hat{\psi}_R(k', t)], \\ &= \left[\int dk \omega^R(k) \hat{\psi}_R(k, t) \hat{\psi}_R^\dagger(k, t), \hat{\psi}_R(k', t) \right], \\ &= \int dk \omega^R(k) [\hat{\psi}_R(k, t) \hat{\psi}_R^\dagger(k, t) \hat{\psi}_R(k', t) - \hat{\psi}_R(k', t) \hat{\psi}_R(k, t) \hat{\psi}_R^\dagger(k, t)], \\ &= \omega^R(k') \hat{\psi}_R(k', t), \end{aligned} \quad (3.25)$$

where we used $[\hat{\psi}_R(k), \hat{\psi}_R^\dagger(k')] = -\delta(k - k')$ together with the continuous antimagnon Hamiltonian which has $\omega^R(k) = JSa^2k^2 - h_R$. These conditions for

the equation of motion derived in (3.24) and (3.25) will thus be applied in section 4.2 in order to properly normalize the different possible magnon, anti magnon and exponential (damped or growing) momentum modes in the full system.

3.5 The Bogoliubov Transformation

The creation and annihilation operators from the Holstein-Primakoff transformation can be expressed in terms of Bogoliubov modes. The usefulness of this lies in the fact that the magnon/antimagnon modes are separated into distinct terms as follows by the Bogoliubov transformation

$$\begin{aligned}\hat{\psi}_L(x, t) &= \int d\omega u_L(x, \omega) \hat{a}_\omega e^{-i\omega t} + v_L^*(x, \omega) \hat{a}_\omega^\dagger e^{i\omega t}, \\ \hat{\psi}_R(x, t) &= \int d\omega v_R(x, \omega) \hat{a}_\omega e^{-i\omega t} + u_R^*(x, \omega) \hat{a}_\omega^\dagger e^{i\omega t}.\end{aligned}\tag{3.26}$$

The operators in (3.26) are the quantum mechanical ladder operators with \hat{a}_ω^\dagger as the creation operator and \hat{a}_ω the annihilation operator. These operators must obey the bosonic commutation relations $[\hat{a}_\omega, \hat{a}_{\omega'}^\dagger] = \delta(\omega - \omega')$ and $[\hat{a}_\omega, \hat{a}_{\omega'}] = [\hat{a}_\omega^\dagger, \hat{a}_{\omega'}^\dagger] = 0$. The $u_{L/R}$ modes describe the magnon modes and $v_{L/R}$ the antimagnon modes. The reason for the switch in what mode precedes which operator, in (3.26) between $\hat{\psi}_L$ and $\hat{\psi}_R$, is to preserve what the magnon/antimagnon modes are. This is evident when we determine the constraints for the definitions made in (3.26). The constraints come from taking the commutation relations for the definitions in (3.26) with the magnon commutation on the left and the antimagnon commutation on the right. This gives the constraint of the Bogoliubov modes on the left and right as seen in equation (3.27)

$$\begin{aligned}[\hat{\psi}_L(x, t), \hat{\psi}_L^\dagger(x', t)] &= \int d\omega u_L(x, \omega) u_L^*(x', \omega) - v_L(x, \omega) v_L^*(x', \omega), \\ &= \delta(x - x'), \\ [\hat{\psi}_R(x, t), \hat{\psi}_R^\dagger(x', t)] &= \int d\omega v_R(x, \omega) v_R^*(x', \omega) - u_R(x, \omega) u_R^*(x', \omega), \\ &= -\delta(x - x').\end{aligned}\tag{3.27}$$

The relations seen in equation (3.27) can be summarized into a singular statement as follows

$$\int d\omega u_{L/R}(x, \omega) u_{L/R}^*(x', \omega) - v_{L/R}(x, \omega) v_{L/R}^*(x', \omega) = \delta(x - x').\tag{3.28}$$

We see from the relation in equation (3.28) that the interpretation of the u/v modes as magnon and antimagnon modes are equivalent on both sides.

Chapter 4

COUPLING THE MAGNON AND ANTIMAGNON REGION

In this chapter we will look at the magnon-antimagnon coupling between the left and right metal. This will result in the derivation of boundary conditions on both sides of the boundary. It will then be possible to apply the Bogoliubov transformation from chapter 3 to the boundary conditions to get the relations between the left and right Bogoliubov modes. These relations will result in the mode matching matrix (M-matrix) which contains all the information of the boundary conditions. This M-matrix will be used to study scattering dynamics in chapter 5.

4.1 Boundary Conditions

In order to determine the scattering dynamics of the (anti)magnons we need to establish the boundary conditions connecting the left and right magnet. This can be done by solving the Heisenberg equation of motion for both sides with the inclusion of a boundary term. The Hamiltonian for the entire system is as follows

$$\begin{aligned}\hat{\mathcal{H}}_{tot} &= -J \sum_{\langle i,j \rangle} \vec{S}_{i,L} \cdot \vec{S}_{j,L} - h_l \sum_i \vec{S}_{i,L}^z - J \sum_{\langle i,j \rangle} \vec{S}_{i,R} \cdot \vec{S}_{j,R} - h_r \sum_j \vec{S}_{j,R}^z \\ &\quad + J' \vec{S}_{B,L} \cdot \vec{S}_{B,R}, \\ &= \hat{\mathcal{H}}_M^L + \hat{\mathcal{H}}_{AM}^R + \hat{\mathcal{H}}_B,\end{aligned}\tag{4.1}$$

with $\hat{\mathcal{H}}_B$ being the boundary term $J' \vec{S}_{B,L} \cdot \vec{S}_{B,R}$ where $J' > 0$. The boundary term now connects both sides at the interface in such a way that anti-alignment between the magnons and antimagnons is the lowest energy contribution possible to the total energy. The Heisenberg equation of motion can be written in the following way

$$-i\partial_t \vec{S}_{B,L/R} = [\hat{\mathcal{H}}_{tot}, \vec{S}_{B,L/R}],\tag{4.2}$$

with the following commutations for the spin vector elements

$$\begin{aligned}[\hat{S}_{i,L/R}^\alpha, \hat{S}_{j,L/R}^\beta] &= i\epsilon^{\alpha\beta\gamma} \hat{S}_{L/R}^\gamma \delta_{i,j}, \\ [\hat{S}_{L/R}^\alpha, \hat{S}_{R/L}^\beta] &= 0.\end{aligned}\tag{4.3}$$

Equations (4.1) and (4.3) can be applied in the Heisenberg equation of motion of the left spin vector.

$$\begin{aligned}
-i\partial_t\vec{S}_{B,L} &= [-J \sum_{\langle i,j \rangle} \vec{S}_{i,L} \cdot \vec{S}_{j,L} + J' \vec{S}_{B,L} \cdot \vec{S}_{B,R} - h_l \sum_i \vec{S}_{i,L}^z, \vec{S}_{B,L}], \\
&= -2J \sum_i [\vec{S}_{i,L} \cdot \vec{S}_{i+1,L}, \vec{S}_{B,L}] + J' [\vec{S}_{B,L} \cdot \vec{S}_{B,R}, \vec{S}_{B,L}] \\
&\quad - h_l \sum_i [\vec{S}_{i,L}^z, \vec{S}_{B,L}], \\
&= -2J [\vec{S}_{B-1,L} \cdot \vec{S}_{B,L}, \vec{S}_{B,L}] + J' [\vec{S}_{B,L} \cdot \vec{S}_{B,R}, \vec{S}_{B,L}] - h_l [\vec{S}_{B,L}^z, \vec{S}_{B,L}], \\
&= i[-2J \vec{S}_{B,L} \times \vec{S}_{B-1,L} + J' \vec{S}_{B,L} \times \vec{S}_{B,R} - h_l \vec{S}_{B,L} \times \vec{S}_{B,L}^z], \\
\partial_t \vec{S}_{B,L} &= 2J \vec{S}_{B,L} \times \vec{S}_{B-1,L} - J' \vec{S}_{B,L} \times \vec{S}_{B,R} + h_l \vec{S}_{B,L} \times \vec{S}_{B,L}^z.
\end{aligned} \tag{4.4}$$

Equation (4.4) describes the boundary conditions in a discretized manner. We want to switch this towards a continuous description since we are gonna use the continuous dispersion relations for the (anti)magnon modes. The continuous version of the left boundary conditions is as follows

$$\begin{aligned}
\partial_t \vec{S}_L(x_B, t) &= \lim_{a \rightarrow 0} 2J [\vec{S}_L(x_B, t) \times \vec{S}_L(x_B - a, t)] \\
&\quad - J' [\vec{S}_L(x_B, t) \times \vec{S}_R(x_B, t)] + h_l [\vec{S}_L(x_B, t) \times \vec{S}_L^z(x_B, t)],
\end{aligned} \tag{4.5}$$

where x_B is the boundary coordinate. It is now possible to approximate $\vec{S}_L(x_B - a, t)$ with the limit of the lattice spacing going to zero as shown below

$$\lim_{a \rightarrow 0} \vec{S}_L(x_B - a, t) = \vec{S}_L(x_B, t) - a \partial_{x_B} \vec{S}_L(x_B, t) + \frac{a^2}{2} \partial_{x_B}^2 \vec{S}_L(x_B, t). \tag{4.6}$$

The relation derived in equation (4.6) can be applied to the continuous boundary conditions in (4.5) resulting in following equation

$$\begin{aligned}
\partial_t \vec{S}_L(x_B, t) &= 2J \vec{S}_L(x_B, t) \times [\vec{S}_L(x_B, t) - a \partial_{x_B} \vec{S}_L(x_B, t) + \frac{a^2}{2} \partial_{x_B}^2 \vec{S}_L(x_B, t)] \\
&\quad - J' [\vec{S}_L(x_B, t) \times \vec{S}_R(x_B, t)] + h_l [\vec{S}_L(x_B, t) \times \vec{S}_L^z(x_B, t)], \\
&= -2Ja [\vec{S}_L(x_B, t) \times \partial_{x_B} \vec{S}_L(x_B, t)] + Ja^2 [\vec{S}_L(x_B, t) \times \partial_{x_B}^2 \vec{S}_L(x_B, t)], \\
&\quad - J' [\vec{S}_L(x_B, t) \times \vec{S}_R(x_B, t)] + h_l [\vec{S}_L(x_B, t) \times \vec{S}_L^z(x_B, t)].
\end{aligned} \tag{4.7}$$

Now all that is left to do is take the cross product of all the spin vectors in equation (4.7). This leaves us with the following equality for the boundary on the left

$$\begin{aligned}
i\partial_t\hat{\psi}_L(x_B, t) = & 2JSa\partial_{x_B}\psi_L(x_B, t) - JSa^2\partial_{x_B}^2\psi_L(x_B, t) \\
& + J'S(\psi_L(x_B, t) + \psi_R(x_B, t)) + h_l\psi_L(x_B, t).
\end{aligned} \tag{4.8}$$

Since we have changed to the continuous field description of the setup it will be necessary to work with the following Fourier transformation of $\psi_L(x_B, t)$

$$\hat{\psi}_L(x_B, t) = \frac{1}{\sqrt{2\pi}} \int dk e^{ikx_B} e^{-i\omega_M^L(k)t} \hat{\psi}_L(k). \tag{4.9}$$

When we apply the time derivative on the Fourier transform of $\hat{\psi}_L(x_B, t)$ in (4.8) we get the first boundary condition

$$\partial_{x_B}\hat{\psi}_L(x_B, t) - \gamma[\hat{\psi}_L(x_B, t) + \hat{\psi}_R(x_B, t)] = 0, \tag{4.10}$$

where $\gamma = \frac{-J'}{2Ja}$. Equation (4.7) also produces the complex conjugated version of (4.10) as seen in equation (4.11)

$$\partial_{x_B}\hat{\psi}_L^\dagger(x_B, t) - \gamma[\hat{\psi}_L^\dagger(x_B, t) + \hat{\psi}_R^\dagger(x_B, t)] = 0. \tag{4.11}$$

The same procedure, used in (4.4) - (4.10), can be applied to the equation of motion of $\vec{S}_{B,R}$. This results in the second set of boundary conditions

$$\partial_{x_B}\hat{\psi}_R(x_B, t) + \gamma[\hat{\psi}_R(x_B, t) + \hat{\psi}_L(x_B, t)] = 0, \tag{4.12a}$$

$$\partial_{x_B}\hat{\psi}_R^\dagger(x_B, t) + \gamma[\hat{\psi}_R^\dagger(x_B, t) + \hat{\psi}_L^\dagger(x_B, t)] = 0. \tag{4.12b}$$

The derived boundary conditions, in equations (4.10)-(4.12b), are similar in structure compared to the classically derived boundary conditions in [2]. The difference is that the classical fields are substituted with quantum mechanical field operators with a different coupling. These boundary conditions convey the physical interpretation that at the boundary creation and annihilation operators couple in such a way that magnons and antimagnons couple between the left and right metal.

4.2 The M-matrix

To determine the scattering amplitudes for all the possible scattering events within the system it is useful to relate all the possible modes within the system in a single equation based upon the boundary conditions in (4.10)-(4.12b). This will be the M-matrix equation. The definitions given in equation (3.26) can be applied to the boundary condition in equation (4.10) to get the boundary conditions for the Bogoliubov modes as shown in equation (4.13)

$$\begin{aligned}
(\partial_{x_B} - \gamma)\hat{\psi}_L(x_B, t) &= \gamma\hat{\psi}_R(x_B, t), \\
(\partial_{x_B} - \gamma) \int d\omega u_L(x_B, \omega)\hat{a}_\omega e^{-i\omega t} + v_L^*(x_B, \omega)\hat{a}_\omega^\dagger e^{i\omega t} &= \\
\gamma \int d\omega v_R(x_B, \omega)\hat{a}_\omega e^{-i\omega t} + u_R^*(x_B, \omega)\hat{a}_\omega^\dagger e^{i\omega t}. &
\end{aligned} \tag{4.13}$$

In order for equation (4.13) to be true for all $t \in [-\infty, \infty]$ it is necessary to separate the terms into relations with the same phase. This results into the following relations

$$\begin{aligned}
(\partial_{x_B} - \gamma)u_L(x_B, \omega) &= \gamma v_R(x_B, \omega), \\
(\partial_{x_B} - \gamma)v_L^*(x_B, \omega) &= \gamma u_R^*(x_B, \omega).
\end{aligned} \tag{4.14}$$

The same can be done for the boundary condition in equation (4.12a) to get

$$\begin{aligned}
-(\partial_{x_B} + \gamma)u_R^*(x_B, \omega) &= \gamma v_L^*(x_B, \omega), \\
-(\partial_{x_B} + \gamma)v_R(x_B, \omega) &= \gamma u_L(x_B, \omega).
\end{aligned} \tag{4.15}$$

The complex conjugated boundary conditions will give the complex conjugated Bogoliubov mode versions of (4.14) and (4.15). In order to compare the same modes left and right it is possible to only take the Bogoliubov modes which are not complex conjugated as follows

$$\begin{aligned}
(\partial_{x_B} - \gamma)u_L(x_B, \omega) &= \gamma v_R(x_B, \omega), \\
(\partial_{x_B} - \gamma)v_L(x_B, \omega) &= \gamma u_R(x_B, \omega), \\
-(\partial_{x_B} + \gamma)u_R(x_B, \omega) &= \gamma v_L(x_B, \omega), \\
-(\partial_{x_B} + \gamma)v_R(x_B, \omega) &= \gamma u_L(x_B, \omega).
\end{aligned} \tag{4.16}$$

The spatial functions for the Bogoliubov modes can be expanded into momentum modes as follows

$$\begin{aligned}
u_{L/R}(x, \omega) &= \sum_i A_{k_i}^{L/R} u_{k_i}^{L/R} e^{ik_i L/R x}, \\
v_{L/R}(x, \omega) &= \sum_i A_{k_i}^{L/R} v_{k_i}^{L/R} e^{ik_i L/R x},
\end{aligned} \tag{4.17}$$

where the u/v momentum modes are determined by equation (4.18). The summation in equation (4.17) runs over $i \in \{l, r, +, -\}$. The equations of motion from (3.24) and (3.25) together with (3.26) gives the following conditions for the Bogoliubov momentum modes

$$\begin{pmatrix} \omega - \omega^{L/R}(k_i) & 0 \\ 0 & \omega + \omega^{L/R}(k_i) \end{pmatrix} \begin{pmatrix} u_{k_i}^{L/R} \\ v_{k_i}^{L/R} \end{pmatrix} = 0. \tag{4.18}$$

All the Bogoliubov momentum modes are explicitly calculated with equation (4.18) and the normalization condition: $||u_{k_i}^{L/R}|^2 - |v_{k_i}^{L/R}|^2| = 1$ in appendix A. The final result of this is shown below

$$\begin{aligned}
u_{k_{l/r}}^L &= 1, & u_{k_{l/r}}^R &= 1, \\
u_{k_{+/-}}^L &= 0, & u_{k_{+/-}}^R &= 0, \\
v_{k_{l/r}}^L &= 0, & v_{k_{l/r}}^R &= 0, \\
v_{k_{+/-}}^L &= 1, & v_{k_{+/-}}^R &= 1.
\end{aligned} \tag{4.19}$$

Equations (4.14) and (4.15) can be combined with (4.17) and (4.19) to arrive at the M matrix equation in (4.20) where $x_B = 0$ is imposed as the final step.

$$\begin{aligned}
W_l \begin{pmatrix} A_R^L \\ A_L^L \\ A_+^L \\ A_-^L \end{pmatrix} &= W_r \begin{pmatrix} A_R^R \\ A_L^R \\ A_+^R \\ A_-^R \end{pmatrix}, \\
\begin{pmatrix} \lambda_r^L & \lambda_l^L & 0 & 0 \\ \gamma & \gamma & 0 & 0 \\ 0 & 0 & \lambda_+^L & \lambda_-^L \\ 0 & 0 & \gamma & \gamma \end{pmatrix} \begin{pmatrix} A_R^L \\ A_L^L \\ A_+^L \\ A_-^L \end{pmatrix} &= \begin{pmatrix} 0 & 0 & \gamma & \gamma \\ 0 & 0 & \lambda_+^R & \lambda_-^R \\ \gamma & \gamma & 0 & 0 \\ \lambda_r^R & \lambda_l^R & 0 & 0 \end{pmatrix} \begin{pmatrix} A_R^R \\ A_L^R \\ A_+^R \\ A_-^R \end{pmatrix},
\end{aligned} \tag{4.20}$$

where $\lambda_j^L = ik_j^L - \gamma$ and $\lambda_j^R = -ik_j^R - \gamma$. The mode matching matrix M is defined as $M = W_r^{-1}W_l$. The inverse of W_r is shown in equation (4.21)

$$W_r^{-1} = \frac{1}{\lambda_l^R - \lambda_r^R} \begin{pmatrix} 0 & 1 \\ 0 & 0 \end{pmatrix} \otimes \begin{pmatrix} \lambda_l^R & -\gamma \\ -\lambda_r^R & \gamma \end{pmatrix} + \frac{1}{\lambda_-^R - \lambda_+^R} \begin{pmatrix} 0 & 0 \\ 1 & 0 \end{pmatrix} \otimes \begin{pmatrix} \lambda_-^R & -\gamma \\ -\lambda_+^R & \gamma \end{pmatrix}. \tag{4.21}$$

This can be multiplied with W_l to derive M as seen in equation (4.22)

$$\begin{aligned}
 M = & \frac{1}{\lambda_l^R - \lambda_r^R} \begin{pmatrix} 0 & 1 \\ 0 & 0 \end{pmatrix} \otimes \begin{pmatrix} \lambda_l^R \lambda_+^L - \gamma^2 & \lambda_l^R \lambda_-^L - \gamma^2 \\ \gamma^2 - \lambda_r^R \lambda_+^L & \gamma^2 - \lambda_r^R \lambda_-^L \end{pmatrix}, \\
 & + \frac{1}{\lambda_l^R - \lambda_r^R} \begin{pmatrix} 0 & 0 \\ 1 & 0 \end{pmatrix} \otimes \begin{pmatrix} \lambda_-^R \lambda_r^L - \gamma^2 & \lambda_-^R \lambda_l^L - \gamma^2 \\ \gamma^2 - \lambda_+^R \lambda_r^L & \gamma^2 - \lambda_+^R \lambda_l^L \end{pmatrix}.
 \end{aligned} \tag{4.22}$$

It is possible to derive the scattering amplitudes from various initial state setups with the M -matrix equation. This will allow us to study the scattering dynamics in this setup and is the stepping stone for chapter 5.

SCATTERING DYNAMICS

In this chapter we will look at so called scattering states, their dynamics and the intricate relations between them. These relations are captured in the scattering matrix (S) which matches in and out states with each other. In order to derive the S matrix it will be necessary to look at probability conservation and symmetries between different in-states.

5.1 Scattering States

It is possible to derive the amplitudes for so called scattering states with the M-matrix. These scattering states are linear combinations of incoming and outgoing plane waves. The in-state is defined as having only one incoming unit amplitude mode (moving towards the boundary) and all outgoing modes (moving away from the boundary). The out-state is defined in the same way as the in-state but with the incoming and outgoing modes switched around. An example of a scattering state will be shown below. The rest of the in/out states are covered in appendix B.

So as an example we will take a look at the in-state $\phi_{R(L)}^{in}$ where R refers to the direction and L the location, with respect to the boundary, of the incoming unit amplitude wave.

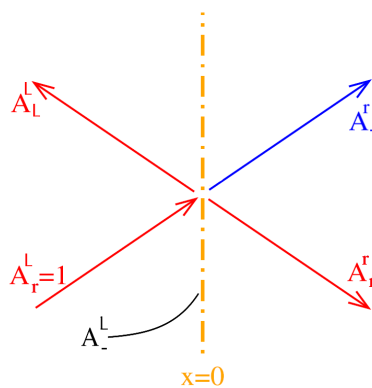


Figure 5.1: In-state $\phi_{R(L)}^{in}$ with unit amplitude A_r^L . Figure adapted from [3].

The colours in figure 5.1, and all other scattering state figures later, refers to the modes being magnonic, antimagnonic or exponentially damped. The red lines will be magnons, the blue lines antimagnons and the black lines exponentially decaying modes. The setup in figure 5.1 can be described in the following way via the M-matrix equation

$$M \begin{pmatrix} 1 \\ A_L^L \\ 0 \\ A_-^L \end{pmatrix} = \begin{pmatrix} A_R^R \\ 0 \\ A_+^R \\ 0 \end{pmatrix}, \quad (5.1)$$

where the two in-states A_L^R and A_-^R are put to zero such that the only incoming state is A_R^L with an amplitude of 1. With the use of the values in the M-matrix it is possible to derive the value's of the amplitudes in this scattering scenario. These amplitudes are described in equation (5.2)

$$\begin{aligned} A_-^L &= 0, \\ A_R^R &= 0, \\ A_L^L &= -\frac{\gamma^2 - \lambda_+^R \lambda_r^L}{\gamma^2 - \lambda_+^R \lambda_l^L} \equiv R, \\ A_+^R &= \frac{1}{\lambda_-^R - \lambda_+^R} [(\lambda_-^R \lambda_r^L - \gamma^2) - \left(\frac{\gamma^2 - \lambda_+^R \lambda_r^L}{\gamma^2 - \lambda_+^R \lambda_l^L}\right)(\lambda_-^R \lambda_l^L - \gamma^2)] \equiv T. \end{aligned} \quad (5.2)$$

We see in (5.2) that the exponential decay mode left and the right moving magnon mode on the right are zero. The only non-zero modes are the reflected magnon mode on the left and the transmitted antimagnon mode on the right. This lines up with the setup of the system that magnons will couple with antimagnons at the boundary.

It is possible to gain more inside into the behaviour and dynamics of these modes by calculating for example $|R|^2$. We do this by multiplying R from (5.2) by it complex conjugation to get

$$|R|^2 = \frac{\gamma^2(h_R - h_L) + \Lambda^{-4}(h_R - \omega)(\omega - h_L) + 2\gamma^2\Lambda^{-2}\sqrt{h_R - \omega}\sqrt{\omega - h_L}}{\gamma^2(h_R - h_L) + \Lambda^{-4}(h_R - \omega)(\omega - h_L) - 2\gamma^2\Lambda^{-2}\sqrt{h_R - \omega}\sqrt{\omega - h_L}}, \quad (5.3)$$

where the momenta from section 3.3 are applied in conjunction with the $\lambda_i^{L/R}$ definitions given in section 4.2. From equation (5.3) we can already deduce an interesting property. This being that for $\omega = h_L$ and $\omega = h_R$ we get that $|R|^2 = 1$. This is to be expected since these two points for ω are the boundaries for magnon-antimagnon coexistence as seen in figure 3.3. Beyond these points we do not have a magnon-antimagnon mode coupling anymore leading to pure magnon reflection. To see the full extend of $|R|^2$ we can look at the plot of equation (5.3) for specific value's of h_L, h_R, γ and Λ . One of such plots is shown in figure 5.2.

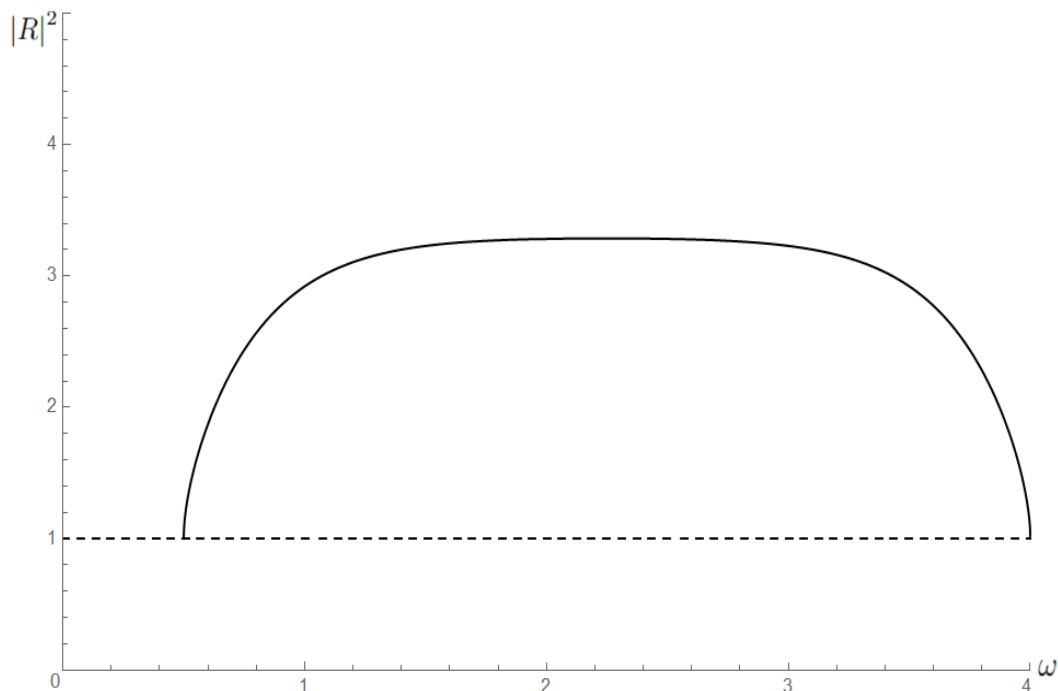


Figure 5.2: Plot of $|R|^2$ with $h_L = 0.5$, $h_R = 4, \gamma = -1$ and $\Lambda = 1$.

It is visible in figure 5.2 that $|R|^2 \geq 1$ for all $\omega \in [h_L, h_R]$. This isn't just an artifact from the chosen parameters in this plot but extends generally for all allowed parameter value's as seen in [2]. This fact ensures that the reflection amplitude will be larger or equal to one for all $\omega \in [h_L, h_R]$. This means that our quantum mechanical treatment of the magnonic analogue of the Klein paradox leads to enhanced magnon spin current just like classically occurs in [2].

When we look at appendix B we see that the scattering from the right $\phi_{-(R)}^{in}$, i.e. the inverted scattering process of $\phi_{R(L)}^{in}$, has the reflection amplitude R' . When we determine $|R'|^2$ with equation (B.1c) it follows that the following relation holds: $|R|^2 = |R'|^2$.

5.2 In and Out States

The in and out states can be described in terms of a more general description of the M-matrix equation. In the initial M-matrix equation we set the plane wave exponential to one since we were looking at the boundary conditions with $x_B = 0$. For the in and out state description it will be necessary to include the plane wave exponential together with the amplitude in order to describe the system as (moving) in/out going plane wave modes. This leads to the following in and out states

$$\phi_{R(L)}^{in}(x, \omega) = \begin{cases} e^{ik_r^l x} + R e^{ik_l^l x} & x < 0, \\ T e^{ik_+^r x} & x > 0, \end{cases} \quad (5.4a)$$

$$\phi_{-(R)}^{in}(x, \omega) = \begin{cases} T' e^{ik_i^l x} & x < 0, \\ e^{ik_-^r x} + R' e^{ik_+^r x} & x > 0, \end{cases} \quad (5.4b)$$

$$\phi_{L(R)}^{in}(x, \omega) = \begin{cases} \tilde{T} e^{ik_-^l x} & x < 0, \\ e^{ik_i^r x} + \tilde{R} e^{ik_r^r x} & x > 0, \end{cases} \quad (5.4c)$$

$$\phi_{L(L)}^{out}(x, \omega) = \begin{cases} e^{ik_i^l x} + R^* e^{ik_r^l x} & x < 0, \\ T^* e^{ik_-^r x} & x > 0, \end{cases} \quad (5.4d)$$

$$\phi_{+(R)}^{out}(x, \omega) = \begin{cases} T'^* e^{ik_r^l x} & x < 0, \\ e^{ik_+^r x} + R'^* e^{ik_-^r x} & x > 0, \end{cases} \quad (5.4e)$$

$$\phi_{R(R)}^{out}(x, \omega) = \begin{cases} \tilde{T}' e^{ik_-^l x} & x < 0, \\ e^{ik_r^r x} + \tilde{R}' e^{ik_i^r x} & x > 0. \end{cases} \quad (5.4f)$$

These in/out states will be used to set up the scattering matrix S which describes the mapping between the in-going and outgoing states. But before deriving the S matrix itself it is beneficial to uncover some symmetries and conservation relations within the system to ease the solvability of the S matrix.

5.3 Conserved Probability Current

When a scattering event takes place there will be various modes present in the system. These modes need to obey so called probability current conservation. The probability current is defined in the following way[4]

$$J(x, \omega) = \frac{-i\hbar}{2m}(\phi^* \partial_x \phi - \phi \partial_x \phi^*), \quad (5.5)$$

where the (x, ω) dependence of ψ is omitted for brevity. For the calculation of the current we ignore the prefactor $\frac{\hbar}{2m}$, where m is the particle mass, since it doesn't influence the final result. The current given in (5.5) can be calculated for any of the defined in/out state functions in (5.4). We will explicitly calculate the conditions for probability current conservation with the scattering setup of $\phi_{R(L)}^{in}(x, \omega)$ in equation (5.4a). The current on the left and right side of the boundary respectively has the following form

$$\begin{aligned} J_L(x < 0, \omega) &= -i(\phi_{R(L)}^{in*} \partial_x \phi_{R(L)}^{in} - \phi_{R(L)}^{in} \partial_x \phi_{R(L)}^{in*}), \\ &= -i[(e^{ik_l^l x} + R^* e^{-ik_l^l x})(-ik_l^l)(e^{-ik_l^l x} + R e^{ik_l^l x}) \\ &\quad - (e^{-ik_l^l x} + R e^{ik_l^l x})(ik_l^l)(e^{ik_l^l x} - R^* e^{-ik_l^l x})], \\ &= -2k_l^l(1 - |R|^2), \end{aligned} \quad (5.6)$$

$$\begin{aligned} J_R(x > 0, \omega) &= -i(\phi_{R(L)}^{in*} \partial_x \phi_{R(L)}^{in} - \phi_{R(L)}^{in} \partial_x \phi_{R(L)}^{in*}), \\ &= -i[(T^* e^{-ik_+^r x} (ik_+^r) T e^{-ik_+^r x}) - (T e^{ik_+^r x} (-ik_+^r) T^* e^{-ik_+^r x})], \\ &= 2k_+^r |T|^2. \end{aligned}$$

These probability currents should be equal at the boundary. This results in the following equality for probability current conservation: $-k_l^l(1 - |R|^2) = k_+^r |T|^2$.

This equality is already quite helpful but not yet in the most useful form. In order to get this into a more use-able form, like a direct amplitude relation, it is possible to normalize the probability currents. This will be done by dividing the currents left and right by the unit amplitude currents for the respective sides. When we do this we get the following relation between scattering amplitudes

$$|R|^2 - |T|^2 = 1. \quad (5.7)$$

This relation between reflection and transmission is crucial for the derivation of the scattering matrix later on in the chapter. It also shows the counter intuitive relation between the incoming and reflected amplitude. When there is any non-zero transmission amplitude leaving the boundary on the right we get by equation (5.7) that the reflection amplitude will be larger than one. This conclusion agrees with what we saw in figure 5.2 where $|R|^2 \geq 1$ for all $\omega \in [h_L, h_R]$. The same current conservation procedure can be done for $\phi_{L(R)}^{in}$ and $\phi_{-(R)}^{in}$. This results in the following relations: $|R'|^2 - |T'|^2 = 1$ and $|\tilde{R}|^2 = 1$. The reason for $\tilde{R} = 1$ is that the incoming magnon mode from the right cannot couple to an antimagnon mode on the left. This leads to the pure reflection of the initial incoming magnon mode.

A final observation is that $|T|^2 = |T'|^2$. We know this because in section 5.1 we concluded that $|R|^2 = |R'|^2$ which can be combined with the conservation relations, $|R|^2 - |T|^2 = 1$ and $|R'|^2 - |T'|^2 = 1$, derived in this section to get the equivalence of the squared norms of the transmissions.

5.4 Solving the S Matrix

There is one particular symmetry hidden within the in and out states that is very useful to uncover for later application. When we take the in-states $\phi_{R(L)}^{in}$ and $\phi_{-(R)}^{in}$ for example it looks like the magnon in-state from the left is a mirror image of the antimagnon in-state from the right. So let's suppose that the in-state $\phi_{-(R)}^{in}$ can be constructed as a linear combination of $\phi_{R(L)}^{in}$ and its complex conjugation. This would take the following form

$$\begin{aligned}
\phi_{-(R)}^{in} &= \frac{1}{T^*} \phi_{R(L)}^{*in} - \frac{R^*}{T^*} \phi_{R(L)}^{in}, \\
&= \begin{cases} \frac{1}{T^*} (e^{ik_l^l x} + R^* e^{ik_r^l x}) - \frac{R^*}{T^*} (e^{ik_r^l x} + R e^{ik_l^l x}) & x < 0, \\ e^{ik_-^r x} - \frac{R^* T}{T^*} e^{ik_+^r x} & x > 0, \end{cases} \\
&= \begin{cases} -T e^{ik_l^l x} & x < 0, \\ e^{ik_-^r x} - \frac{R^* T}{T^*} e^{ik_+^r x} & x > 0, \end{cases} \quad (5.8) \\
&= \begin{cases} T' e^{ik_l^l x} & x < 0, \\ e^{ik_-^r x} + R' e^{ik_l^l x} & x > 0, \end{cases}
\end{aligned}$$

where the prefactors are chosen in such a way that the phase exponents can be compared. From the second to third equivalence the norm, $|R|^2 - |T|^2 = 1$, was applied in the upper line for $x < 0$. The matching of plane wave phases

leads to the following two relations

$$T' = -T, \quad R'T^* + R^*T = 0. \quad (5.9)$$

With the relations from (5.9) and section 5.3 it is possible to set up the scattering matrix by relating the in/out states. The way to approach this is to take a set of in-going and outgoing unit amplitude plane waves as follows

$$\vec{I} = \begin{pmatrix} I_M^L \\ I_M^R \\ I_{AM}^R \end{pmatrix} = \begin{pmatrix} e^{ik_r^l x} \Theta(-x) \\ e^{ik_l^r x} \Theta(x) \\ e^{ik^r_- x} \Theta(x) \end{pmatrix}, \quad (5.10a)$$

$$\vec{O} = \begin{pmatrix} O_M^L \\ O_M^R \\ O_{AM}^R \end{pmatrix} = \begin{pmatrix} e^{ik_l^l x} \Theta(-x) \\ e^{ik_r^r x} \Theta(x) \\ e^{ik^r_+ x} \Theta(x) \end{pmatrix}, \quad (5.10b)$$

where the subscript indicates whether it is a magnon or antimagnon mode. The $\Theta(x)$ function represents the Heaviside step function for $x \in \{-\infty, \infty\}$. The in/out states from (5.4) can be written in a similar fashion with the Heaviside step function.

We now make the ansatz that the in/out states can be expressed by linear combinations of (5.10a) and (5.10b) with the scattering matrix S . This will give the following equations

$$\begin{pmatrix} \phi_{R(L)}^{in} \\ \phi_{L(R)}^{in} \\ \phi_{-(R)}^{in} \end{pmatrix} = \vec{I} + S\vec{O}, \quad (5.11a)$$

$$\begin{pmatrix} \phi_{L(L)}^{out} \\ \phi_{R(R)}^{out} \\ \phi_{+(R)}^{out} \end{pmatrix} = \vec{O} + S'\vec{I}. \quad (5.11b)$$

The inspiration for equations (5.8), (5.10a/b) and (5.11a/b) comes from [5]. With the full expressions of the in and out states, in equations (5.4a)-(5.4f), in terms of $\Theta(x)$ functions it is possible to derive what the S and S' matrix entries are when looking at $x < 0$ and $x > 0$. This procedure results in the following two scattering matrices

$$S = \begin{pmatrix} R & 0 & T \\ 0 & 1 & 0 \\ T' & 0 & R' \end{pmatrix}, \quad S' = \begin{pmatrix} R^* & 0 & T^* \\ 0 & 1 & 0 \\ T'^* & 0 & R'^* \end{pmatrix}. \quad (5.12)$$

It is immediately obvious that $S' = S^*$. We can substitute equation (5.11a) into equation (5.11b) to directly relate the in and out states to each other

$$\begin{pmatrix} \phi_{L(L)}^{out} \\ \phi_{R(R)}^{out} \\ \phi_{+(R)}^{out} \end{pmatrix} = \vec{O}(\mathbb{I}_{3 \times 3} - S^*S) + S^* \begin{pmatrix} \phi_{R(L)}^{in} \\ \phi_{L(R)}^{in} \\ \phi_{-(R)}^{in} \end{pmatrix}. \quad (5.13)$$

Equation (5.13) shows that $\vec{\phi}^{out}$ is directly related to $\vec{\phi}^{in}$ by the complex conjugated S matrix if $S^*S = \mathbb{I}_{3 \times 3}$. So we calculate S^*S in equation (5.14) to check whether or not this is the case.

$$\begin{aligned} S^*S &= \begin{pmatrix} R^* & 0 & T^* \\ 0 & 1 & 0 \\ T'^* & 0 & R'^* \end{pmatrix} \begin{pmatrix} R & 0 & T \\ 0 & 1 & 0 \\ T' & 0 & R' \end{pmatrix}, \\ &= \begin{pmatrix} RR^* + T^*T' & 0 & R^*T + R'T^* \\ 0 & 1 & 0 \\ T'^*R + R'^*T' & 0 & T'^*T + R'^*R' \end{pmatrix}, \\ &= \begin{pmatrix} |R|^2 - |T|^2 & 0 & R^*T + R'T^* \\ 0 & 1 & 0 \\ -T^*R - R'^*T & 0 & |R'|^2 - |T'|^2 \end{pmatrix}. \end{aligned} \quad (5.14)$$

From the second to third equality, in equation (5.14), we used the relation $T' = -T$ from (5.9). We see that $S^*S = \mathbb{I}_{3 \times 3}$ at all times when the relations from (5.9) together with $|R|^2 - |T|^2 = 1$ and $|R'|^2 - |T'|^2 = 1$ are applied to the final equality of (5.14). One curious thing to notice about the S matrix is that it seems to break unitarity since $SS^\dagger \neq \mathbb{I}_{3 \times 3}$. The reason for this apparent break is that $SS^\dagger = \mathbb{I}_{3 \times 3}$ isn't the unitarity condition for this system. We instead have $S\eta S^\dagger = \eta$ with $\eta = \text{diag}(1,1,-1)$ as the unitarity condition which is satisfied by S given in equation (5.12).

The fact that $S^*S = \mathbb{I}_{3 \times 3}$ leads to the following relation for the in and out states from equation (5.13)

$$\begin{pmatrix} \phi_{L(L)}^{out} \\ \phi_{R(R)}^{out} \\ \phi_{+(R)}^{out} \end{pmatrix} = \begin{pmatrix} R^* & 0 & T^* \\ 0 & 1 & 0 \\ T'^* & 0 & R'^* \end{pmatrix} \begin{pmatrix} \phi_{R(L)}^{in} \\ \phi_{L(R)}^{in} \\ \phi_{-(R)}^{in} \end{pmatrix}. \quad (5.15)$$

So equation (5.15) contains all the information relating the in/out state functions via the S matrix. The S matrix is essential to derive the (anti)magnonic

number operator for spontaneous (anti)magnon emission. For these occupation numbers we do not need in/out state functions by themselves but in/out state operators. This means that the in/out state operator will work on some initial state to create or destroy the in/out state functions via ladder operators just like the Bogoliubov ladder operators. The in and out states operators are defined in the following way

$$\begin{aligned}
\hat{\phi}_{L(L)}^{out}(x, \omega) &\equiv \phi_{L(L)}^{out}(x, \omega) \hat{a}_{\omega, L(L)}^{out}, \\
\hat{\phi}_{R(R)}^{out}(x, \omega) &\equiv \phi_{R(R)}^{out}(x, \omega) \hat{a}_{\omega, R(R)}^{out}, \\
\hat{\phi}_{+(R)}^{out}(x, \omega) &\equiv \phi_{+(R)}^{out}(x, \omega) \hat{a}_{\omega, +(R)}^{\dagger out}, \\
\hat{\phi}_{R(L)}^{in}(x, \omega) &\equiv \phi_{R(L)}^{in}(x, \omega) \hat{a}_{\omega, R(L)}^{in}, \\
\hat{\phi}_{L(R)}^{in}(x, \omega) &\equiv \phi_{L(R)}^{in}(x, \omega) \hat{a}_{\omega, L(R)}^{in}, \\
\hat{\phi}_{-(R)}^{in}(x, \omega) &\equiv \phi_{-(R)}^{in}(x, \omega) \hat{a}_{\omega, -(R)}^{\dagger in},
\end{aligned} \tag{5.16}$$

where $[\hat{a}_{\omega, \mu}^{\nu}, \hat{a}_{\omega', \mu'}^{\dagger \nu'}] = \delta(\omega - \omega') \delta_{\mu, \mu'} \delta_{\nu, \nu'}$ and $[\hat{a}_{\omega, \mu}^{\nu}, \hat{a}_{\omega, \mu'}^{\nu'}] = [\hat{a}_{\omega, \mu}^{\dagger \nu}, \hat{a}_{\omega', \mu'}^{\dagger \nu'}] = 0$. The indices are defined as: $\mu \in \{L(L), R(L), L(R), R(R), +(R), -(R)\}$ and $\nu \in \{\text{in}, \text{out}\}$. The peculiar thing to notice about the definitions in (5.16) is that $\hat{\phi}_{-(R)}^{\dagger in}$ and $\hat{\phi}_{+(R)}^{out}$ come with a creation ladder operator rather than an annihilation ladder operator like the other in/out state operators. The reason for this is that the antimagnon states on the right are characterized by a negative norm. This forces the definition to have the creation ladder operator for initial antimagnon states and an annihilation ladder operator for initial magnon states.

With the definitions given in (5.16) we can relate the creation and annihilation ladder operators of the in and out state operators as follows

$$\begin{pmatrix} \hat{a}_{\omega, L(L)}^{out} \\ \hat{a}_{\omega, R(R)}^{out} \\ \hat{a}_{\omega, +(R)}^{\dagger out} \end{pmatrix} = \begin{pmatrix} R^* & 0 & T^* \\ 0 & 1 & 0 \\ T'^* & 0 & R'^* \end{pmatrix} \begin{pmatrix} \hat{a}_{\omega, R(L)}^{in} \\ \hat{a}_{\omega, L(R)}^{in} \\ \hat{a}_{\omega, -(R)}^{\dagger in} \end{pmatrix}. \tag{5.17}$$

The relations between the in/out state ladder operators will be used in the next chapter about spontaneous (anti)magnon emission.

SPONTANEOUS MAGNONIC EMISSION

In this chapter we will cover how the mixing of creation and annihilation operators in equation (5.17) leads to spontaneous magnon emission in an in-state vacuum. In addition to this we will also cover how the extension to thermal in-states looks like with respect to the vacuum in-state and at which critical temperature the spontaneous emission isn't separable from the thermal emission.

6.1 Magnonic Particle Numbers

Everything discussed thus far has been the result of stimulated emission. This means that some initial (anti)magnonic interacts with the system. This leads to the various scattering events seen in the in/out state figures 5.1 and B.1-B.5. Another possible scenario to look at is spontaneous emission. For this type of emission there is no need for any initial incoming state to cause a reaction from the system. To figure out if this system has such emission we have the following definition for the (anti)magnon particle number [3]

$$n_L^L(\omega) \equiv \langle 0, in | \hat{a}_{\omega, L(L)}^{\dagger out} \hat{a}_{\omega, L(L)}^{out} | 0, in \rangle, \quad (6.1)$$

$$n_+^R(\omega) \equiv \langle 0, in | \hat{a}_{\omega, +(R)}^{\dagger out} \hat{a}_{\omega, +(R)}^{out} | 0, in \rangle.$$

The in-state vacuum $|0, in\rangle$, used in equation (6.1), is defined as $\hat{a}_{\omega, x}^{in} |0, in\rangle = 0$ where $x \in \{R(L), (L(R)), -(R)\}$ and $\langle 0, in | 0, in \rangle = 1$. This means that the in-state vacuum $|0, in\rangle$ has no incoming waves going to the boundary. It is possible to rewrite the out state creation and annihilation operators in definition (6.1) with the relations given in equation (5.17). When we do this we get the particle number $n_L^L(\omega)$ on the left side of the boundary and $n_+^R(\omega)$ on the right side of the boundary.

These quantities are given in equation (6.2)

$$\begin{aligned}
n_L^L(\omega) &\equiv \langle 0, in | \hat{a}_{\omega, L(L)}^{\dagger out} \hat{a}_{\omega, L(L)}^{out} | 0, in \rangle, \\
&= \langle 0, in | (R \hat{a}_{\omega, R(L)}^{\dagger in} + T \hat{a}_{\omega, -(R)}^{\dagger in}) (R^* \hat{a}_{\omega, R(L)}^{in} + T^* \hat{a}_{\omega, -(R)}^{\dagger in}) | 0, in \rangle, \\
&= |R|^2 \langle 0, in | \hat{a}_{\omega, R(L)}^{\dagger in} \hat{a}_{\omega, R(L)}^{in} | 0, in \rangle + |T|^2 \langle 0, in | \hat{a}_{\omega, -(R)}^{in} \hat{a}_{\omega, -(R)}^{\dagger in} | 0, in \rangle \\
&+ RT^* \langle 0, in | \hat{a}_{\omega, R(L)}^{\dagger in} \hat{a}_{\omega, -(R)}^{\dagger in} | 0, in \rangle + R^* T \langle 0, in | \hat{a}_{\omega, -(R)}^{in} \hat{a}_{\omega, R(L)}^{in} | 0, in \rangle, \\
&= |T|^2 \langle 0, in | \hat{a}_{\omega, -(R)}^{in} \hat{a}_{\omega, -(R)}^{\dagger in} | 0, in \rangle, \\
&= |T|^2. \\
\\
n_+^R(\omega) &\equiv \langle 0, in | \hat{a}_{\omega, +(R)}^{\dagger out} \hat{a}_{\omega, +(R)}^{out} | 0, in \rangle, \\
&= \langle 0, in | (T'^* \hat{a}_{\omega, R(L)}^{in} + R'^* \hat{a}_{\omega, -(R)}^{\dagger in}) (T' \hat{a}_{\omega, R(L)}^{\dagger in} + R' \hat{a}_{\omega, -(R)}^{in}) | 0, in \rangle, \\
&= |R'|^2 \langle 0, in | \hat{a}_{\omega, -(R)}^{\dagger in} \hat{a}_{\omega, -(R)}^{in} | 0, in \rangle + |T'|^2 \langle 0, in | \hat{a}_{\omega, R(L)}^{in} \hat{a}_{\omega, R(L)}^{\dagger in} | 0, in \rangle \\
&+ R' T'^* \langle 0, in | \hat{a}_{\omega, R(L)}^{in} \hat{a}_{\omega, -(R)}^{\dagger in} | 0, in \rangle + R'^* T' \langle 0, in | \hat{a}_{\omega, -(R)}^{\dagger in} \hat{a}_{\omega, R(L)}^{in} | 0, in \rangle, \\
&= |T'|^2 \langle 0, in | \hat{a}_{\omega, R(L)}^{in} \hat{a}_{\omega, R(L)}^{\dagger in} | 0, in \rangle, \\
&= |T'|^2.
\end{aligned} \tag{6.2}$$

We see that the system has a non-zero value for the particle numbers on the left and right side in equation (6.2) if $h_L < \omega < h_R$. These non-zero particle numbers arise due to the mixing of creation and annihilation operators in (5.17). This means that the system generates spontaneous emission. From equation (6.2) it follows that the spontaneous emission on the left and the right are equal since $|T|^2 = |T'|^2$ as was concluded in section 5.3. The equality of the particle numbers stems from the fact that the magnons and antimagnons are coupled at the boundary. When a quantum fluctuation around the vacuum on one side generates a flux of (anti)magnons then the coupling will generate an equal flux on the other side to get conservation of energy.

6.2 Thermal in-states

We have worked thus far with the in-state vacuum at absolute zero. In any physical setup it will not be possible to prepare the system at absolute system in order to measure the spontaneous emission. To get a more realistic system setup it is possible to introduce a thermal in-state. This thermal in-state will be an in-state caused by thermal fluctuations at a non zero temperature. We will take a look at the thermal in-state coming from the left ($\phi_{R(L)}^{in}$). So to set up this thermal in-state we define the occupied states, adapted from chapter 6 in [6], build upon the in-state vacuum

as follows

$$|n\rangle = \frac{(\hat{a}_{R(L)}^{in\dagger})^n}{\sqrt{n!}} |0, in\rangle. \quad (6.3)$$

These occupation states will be applied in the Boltzmann distributed density matrix ρ . This density matrix ρ is defined below

$$\rho = \frac{1}{Z} \sum_{n=0}^{\infty} e^{-\beta\hbar\omega n} |n\rangle \langle n|, \quad (6.4)$$

where $\beta \equiv \frac{1}{k_b T}$ and the orthogonal states, $\langle n|n'\rangle = 0$ when $n \neq n'$, are already removed. The partition function is defined as follows: $Z = \sum_{n=0}^{\infty} e^{-\beta\hbar\omega n}$. With the density matrix defined in (6.4) we get to the definition for the thermal average as follows

$$\langle \hat{O} \rangle_T = Tr[\hat{O}\rho] = \frac{1}{Z} \sum_{n=0}^{\infty} e^{-\beta\hbar\omega n} \langle n| \hat{O} |n\rangle, \quad (6.5)$$

where Tr is the trace. The definitions given in (6.4) and (6.5) are adapted from chapter 4 in [6]. With these definitions we can calculate the thermal particle number $n_{L,T}^L(\omega)$.

$$\begin{aligned} n_{L,T}^L(\omega) &= \frac{1}{Z} \sum_{n=0}^{\infty} \frac{e^{-\beta\hbar\omega n}}{n!} \langle 0, in | (\hat{a}_{R(L)}^{in})^n (\hat{a}_{\omega,L(L)}^{\dagger out}) \hat{a}_{\omega,L(L)}^{out} (\hat{a}_{R(L)}^{in\dagger})^n |0, in\rangle, \\ &= |T|^2 + \frac{|R|^2}{e^{\beta\hbar\omega} - 1}. \end{aligned} \quad (6.6)$$

From equation (6.6) we see that in addition to the $|T|^2$ in the absolute zero case we also get $|R|^2$ times the Bose-Einstein distribution from the thermal in-state. The reason that the Bose-Einstein distribution appears is due to the (anti)magnons being bosonic excitation's. Whenever one would take the temperature limit going to absolute zero for $n_{L,T}^L(\omega)$ it follows that the original $n_L^L(\omega)$ is retrieved.

Since we have derived the particle number for a thermal in-state it is possible to compare the contributions of the spontaneous emission with the thermal emission. We can say that there isn't any possible distinction left between both contributions when they are equal. From this it is possible to derive a critical temperature such that both contributions are equal as shown in equation (6.7)

$$\begin{aligned} |T|^2 &= \frac{|R|^2}{e^{\beta_c \hbar\omega} - 1}, \\ T_c &= \frac{\hbar\omega}{k_b} \ln\left(1 + \frac{|R|^2}{|T|^2}\right)^{-1}, \\ &= \frac{\hbar\omega}{k_b} \ln\left(\frac{2|R|^2 - 1}{|R|^2 - 1}\right)^{-1}. \end{aligned} \quad (6.7)$$

The third equality in equation (6.7) is obtained by applying $|R|^2 - |T|^2 = 1$. The prefactor of T_c can give a starting point for the order of magnitude of the critical temperature. In this magnonic setup we have ω in the GHz range. When we calculate the prefactor then with the value's of \hbar and k_b we get T_c in the order of magnitude of milikelvin. The inverse natural log in equation (6.7) has a maximum value of $\ln 2^{-1}$. The order of magnitude of T_c could get into the Kelvin range if ω almost gets to THz order. The stability of the system should be studied carefully to see if THz frequencies are feasible to access.

CONCLUSION AND OUTLOOK

In this chapter we will re-summarize the derived results in the form of a conclusion and an outlook on future possibilities within this thesis project.

7.1 Conclusion

In this thesis we have derived a similar M-matrix with respect to [2]. The key element of enhanced magnon spin current, $R \geq 1$, is also found in the quantum mechanical treatment of the magnonic Klein paradox.

We have seen furthermore that, for $h_L < \omega < h_R$, there is spontaneous (anti)magnon emission from the boundary on both sides while being in the in-state vacuum. This spontaneous emission shows itself in the form of the particle numbers as follows: $n_L^L(\omega) = n_+^R(\omega) = |T|^2$.

When we introduce thermal in-states in the system we get an additional contribution to the particle number as follows: $n_{L,T}^L(\omega) = |T|^2 + \frac{|R|^2}{e^{\beta\hbar\omega} - 1}$. This thermal contribution allowed the computation of the critical temperature such that the spontaneous and thermal emission are equal. This critical temperature is $T_c = \frac{\hbar\omega}{k_b} \ln(1 + \frac{|R|^2}{|T|^2})^{-1}$.

7.2 Outlook

Within this thesis there are certain assumptions made and properties left unexplored. The first thing that can be expanded upon is introducing higher order interactions for (anti)magnons in chapter 3. We now only looked at the freely moving (anti)magnon excitation's and not the interactions that they will have with each other.

Two potentially interesting properties left unexplored in this thesis are the density-density correlation functions and the quantum entanglement between the spontaneously emitted magnon/antimagnon pairs. These properties would potentially give some insight into the measurability of the spontaneous emission and the entanglement between them with possible application for quantum computing.

One final idea would be to try and modify the system such that it has a (effectively) linear dispersion. With this it might be possible to create a magnonic black hole and identify the potential spontaneous emission as Hawking radiation with inspiration from [9].

A p p e n d i x A

BOGOLIUBOV MOMENTUM MODES

In this section there will be a derivation of the momentum modes $u_{k_i}^{L/R}$ and $v_{k_i}^{L/R}$ found in equation (4.17). The momentum modes can be determined by applying the Bogoliubov modes from equation (3.26) on the equations of motion in (3.24) and (3.25) with the use of $\omega^L(k) = JSa^2k^2 + h_L$ and $\omega^R(k) = JSa^2k^2 - h_R$. This results in the following two sets of equations

$$\begin{pmatrix} \omega - (JSa^2k_i^2 + h_L) & 0 \\ 0 & \omega + (JSa^2k_i^2 + h_L) \end{pmatrix} \begin{pmatrix} u_{k_i}^L \\ v_{k_i}^L \end{pmatrix} = 0, \quad (\text{A.1a})$$

$$\begin{pmatrix} \omega + (-JSa^2k_i^2 + h_R) & 0 \\ 0 & \omega - (-JSa^2k_i^2 + h_R) \end{pmatrix} \begin{pmatrix} u_{k_i}^R \\ v_{k_i}^R \end{pmatrix} = 0. \quad (\text{A.1b})$$

The specific momenta derived in section 3.3 can be plugged into (A.1a) and (A.1b). This yields the sets of equations described in (A.2) - (A.5). The momentum modes have to satisfy these given equations as well as normalization with respect to the following definition: $||u_{k_i}^{L/R}|^2 - |v_{k_i}^{L/R}|^2| = 1$.

$$\begin{aligned} & \begin{pmatrix} \omega - (JSa^2k_{l/r}^2 + h_L) & 0 \\ 0 & \omega + (JSa^2k_{l/r}^2 + h_L) \end{pmatrix} \begin{pmatrix} u_{k_{l/r}}^L \\ v_{k_{l/r}}^L \end{pmatrix} = 0, \\ & \begin{pmatrix} \omega - (\omega - h_L + h_L) & 0 \\ 0 & \omega + (\omega - h_L + h_L) \end{pmatrix} \begin{pmatrix} u_{k_{l/r}}^L \\ v_{k_{l/r}}^L \end{pmatrix} = 0, \\ & \begin{pmatrix} 0 & 0 \\ 0 & 2\omega \end{pmatrix} \begin{pmatrix} u_{k_{l/r}}^L \\ v_{k_{l/r}}^L \end{pmatrix} = 0, \\ & v_{k_{l/r}}^L = 0, \quad u_{k_{l/r}}^L = 1. \end{aligned} \quad (\text{A.2})$$

$$\begin{aligned} & \begin{pmatrix} \omega - (JSa^2k_{+/-}^2 + h_L) & 0 \\ 0 & \omega + (JSa^2k_{+/-}^2 + h_L) \end{pmatrix} \begin{pmatrix} u_{k_{+/-}}^L \\ v_{k_{+/-}}^L \end{pmatrix} = 0, \\ & \begin{pmatrix} \omega - (-\omega - h_L + h_L) & 0 \\ 0 & \omega + (-\omega - h_L + h_L) \end{pmatrix} \begin{pmatrix} u_{k_{+/-}}^L \\ v_{k_{+/-}}^L \end{pmatrix} = 0, \\ & \begin{pmatrix} 2\omega & 0 \\ 0 & 0 \end{pmatrix} \begin{pmatrix} u_{k_{+/-}}^L \\ v_{k_{+/-}}^L \end{pmatrix} = 0, \\ & v_{k_{+/-}}^L = 1, \quad u_{k_{+/-}}^L = 0. \end{aligned} \quad (\text{A.3})$$

$$\begin{aligned}
& \begin{pmatrix} \omega + (-JSa^2k_{l/r}^2 + h_R) & 0 \\ 0 & \omega - (-JSa^2k_{l/r}^2 + h_R) \end{pmatrix} \begin{pmatrix} u_{k_{l/r}}^R \\ v_{k_{l/r}}^R \end{pmatrix} = 0, \\
& \begin{pmatrix} \omega + (-\omega - h_R + h_R) & 0 \\ 0 & \omega - (-\omega - h_R + h_R) \end{pmatrix} \begin{pmatrix} u_{k_{l/r}}^R \\ v_{k_{l/r}}^R \end{pmatrix} = 0, \\
& \begin{pmatrix} 0 & 0 \\ 0 & 2\omega \end{pmatrix} \begin{pmatrix} u_{k_{l/r}}^R \\ v_{k_{l/r}}^R \end{pmatrix} = 0, \\
& v_{k_{l/r}}^R = 0, \quad u_{k_{l/r}}^R = 1.
\end{aligned} \tag{A.4}$$

$$\begin{aligned}
& \begin{pmatrix} \omega + (-JSa^2k_{+/-}^2 + h_R) & 0 \\ 0 & \omega - (-JSa^2k_{+/-}^2 + h_R) \end{pmatrix} \begin{pmatrix} u_{k_{+/-}}^R \\ v_{k_{+/-}}^R \end{pmatrix} = 0, \\
& \begin{pmatrix} \omega + (\omega - h_R + h_R) & 0 \\ 0 & \omega - (\omega - h_R + h_R) \end{pmatrix} \begin{pmatrix} u_{k_{+/-}}^R \\ v_{k_{+/-}}^R \end{pmatrix} = 0, \\
& \begin{pmatrix} 2\omega & 0 \\ 0 & 0 \end{pmatrix} \begin{pmatrix} u_{k_{+/-}}^R \\ v_{k_{+/-}}^R \end{pmatrix} = 0, \\
& v_{k_{+/-}}^R = 1, \quad u_{k_{+/-}}^R = 0.
\end{aligned} \tag{A.5}$$

The value's for the u/v momentum modes will be applied when deriving the M-matrix.

A p p e n d i x B

SCATTERING STATES

In this section all the other scattering states, that weren't covered in the main text, are shown graphically in figures B.1-B.5. These figures are adapted from Faccio[3]. After the figures we have table B.1 where we see all the amplitudes present in the setup for various initial states. The explicit value's of these amplitudes are shown in equations (B.1a)-(B.1h).

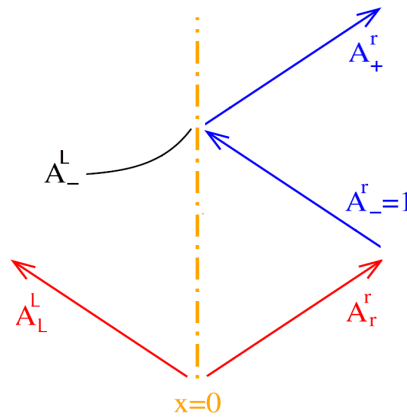


Figure B.1: In-state $\phi_{-(R)}^{in}$ with unit amplitude A_-^R .

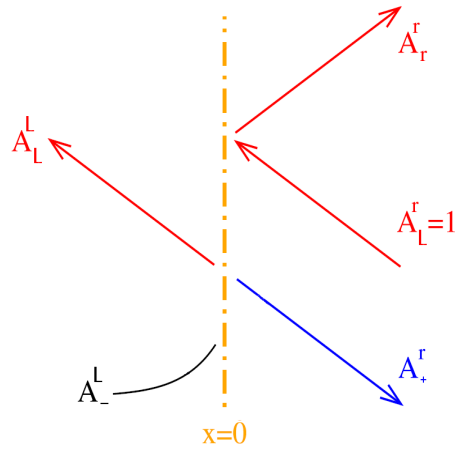


Figure B.2: In-state $\phi_{L(R)}^{in}$ with unit amplitude A_L^R .

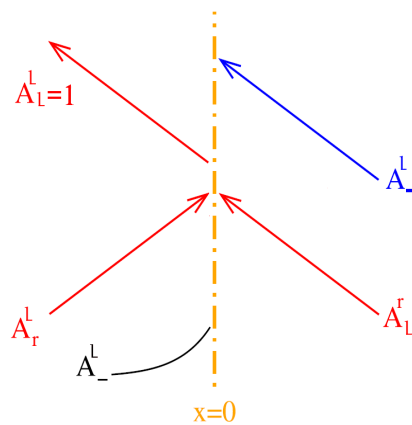


Figure B.3: Out-state $\phi_{L(L)}^{out}$ with unit amplitude A_L^L .

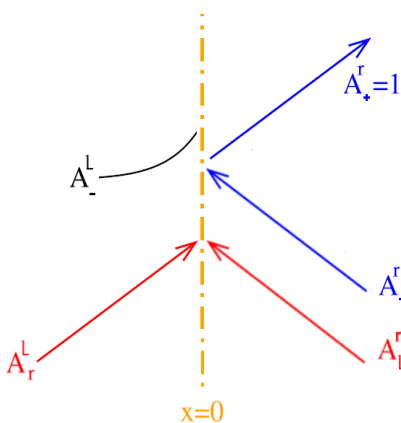


Figure B.4: Out-state $\phi_{+(R)}^{out}$ with unit amplitude A_+^R .

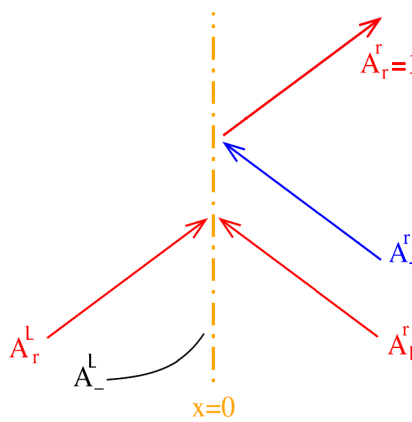


Figure B.5: Out-state $\phi_{R(R)}^{out}$ with unit amplitude A_R^R .

	A_R^L	A_L^L	A_+^L	A_-^L	A_R^R	A_L^R	A_+^R	A_-^R
$\phi_{R(L)}^{in}$	1	R	0	0	0	0	T	0
$\phi_{L(R)}^{in}$	0	0	0	\tilde{T}	\tilde{R}	1	0	0
$\phi_{-(R)}^{in}$	0	T'	0	0	0	0	R'	1
$\phi_{L(L)}^{out}$	R^*	1	0	0	0	0	0	T^*
$\phi_{R(R)}^{out}$	0	0	0	\tilde{T}'	1	\tilde{R}'	0	0
$\phi_{+(R)}^{out}$	T'^*	0	0	0	0	0	1	R'^*

Table B.1: All the amplitudes present in a specific in/out state.

$$R = -\frac{\gamma^2 - \lambda_+^R \lambda_r^L}{\gamma^2 - \lambda_+^R \lambda_l^L}, \quad (\text{B.1a})$$

$$T = \frac{1}{\lambda_-^R - \lambda_+^R} [(\lambda_-^R \lambda_r^L - \gamma^2) - (\frac{\gamma^2 - \lambda_+^R \lambda_r^L}{\gamma^2 - \lambda_+^R \lambda_l^L})(\lambda_-^R \lambda_l^L - \gamma^2)], \quad (\text{B.1b})$$

$$R' = -\frac{\gamma^2 - \lambda_-^R \lambda_l^L}{\gamma^2 - \lambda_+^R \lambda_l^L}, \quad (\text{B.1c})$$

$$T' = \frac{\lambda_-^R - \lambda_+^R}{\gamma^2 - \lambda_+^R \lambda_l^L}, \quad (\text{B.1d})$$

$$\tilde{T} = \frac{\lambda_l^R - \lambda_r^R}{\gamma^2 - \lambda_r^R \lambda_-^L}, \quad (\text{B.1e})$$

$$\tilde{R} = -\frac{\gamma^2 - \lambda_l^R \lambda_-^L}{\gamma^2 - \lambda_r^R \lambda_-^L}, \quad (\text{B.1f})$$

$$\tilde{T}' = \frac{\lambda_l^R - \lambda_r^R}{\lambda_l^R \lambda_-^L - \gamma^2}, \quad (\text{B.1g})$$

$$\tilde{R}' = -\frac{\gamma^2 - \lambda_r^R \lambda_-^L}{\gamma^2 - \lambda_l^R \lambda_-^L}. \quad (\text{B.1h})$$

BIBLIOGRAPHY

- [1] A. Auerbach, "*Interacting Electrons and Quantum Magnetism*", Springer, 1994, Section: 7.1 and 11.2.
- [2] J.S. Harms, H.Y. Yuan, R.A. Duine, "*Enhanced magnon spin current using the bosonic Klein paradox*", URL <https://arxiv.org/pdf/2109.00865.pdf>, 8-02-2022.
- [3] D. Faccio, "*Analogue Gravity Phenomenology*", Springer, 2013, Chapter 9.
- [4] D.J. Griffiths, "*Introduction to Quantum Mechanics second edition*", Pearson, 2004, Chapter 1.
- [5] D.Tong, "*Lectures on Applications of Quantum Mechanics*", University of Cambridge, Chapter 10: scattering theory, URL <https://www.damtp.cam.ac.uk/user/tong/aqm/aqmten.pdf>.
- [6] H.T.C. Stoof, K.B. Gubbels, D.B.M. Dickerscheid, "*Ultracold Quantum Fields*", Springer, 2009, Chapter 3,4 and 6.
- [7] Sebastian Wintz, Vasil Tiberkevich, Markus Weigand, Jörg Raabe, Jürgen Lindner, Artur Erbe, Andrei Slavin Jürgen Fassbender, "*Magnetic vortex cores as tunable spin-wave emitters*", Nature Nanotechnology volume 11, p. 948–953, 2016.
- [8] Johannes Gutenberg University Mainz, "*Spin-Orbit Torques in Various Multilayers*", URL: <https://www.klaui-lab.physik.uni-mainz.de/spin-orbit-torques-in-various-multilayers>.
- [9] A. Roldan-Molina, A.S. Nunez, and R.A. Duine, "*Magnonic black holes*", URL <https://arxiv.org/pdf/1610.02313.pdf>, 7-10-2016.